Supplementary Information for

Approaching an Adjustable Organic Thermochromic Luminophore Library via the Synergistic Effects between Structure-Related Molecule Dynamics and Aggregation-Related Luminescence

Rui Liao,[a] Sen Gu,[a] Xiumei Wang,[a] Xinglin Zhang,[a] Xiaoji Xie,[a] Huibin Sun, *[a,c] Wei Huang*[ab]

[a]China Key Laboratory of Flexible Electronics (KLOFE) & Institute of Advanced Materials (IAM), Jiangsu National Synergistic Innovation Center for Advanced Materials (SICAM), Nanjing Tech University (NanjingTech), 30 South Puzhu Road, Nanjing 211816, P.R. China.

[b]Shaanxi Institute of Flexible Electronics (SIFE), Northwestern Polytechnical University (NPU), 127 West Youyi Road, Xi'an 710072, China.

[c]Jiangsu Key Laboratory for Biosensors, Institute of Advanced Materials (IAM), Nanjing University of Posts and Telecommunications, 9 Wenyuan Road, Nanjing 210023, China.

*Corresponding authors E-mail: iamhbsun@njtech.edu.cn

Methods

General. Unless otherwise noted, all starting materials and reagents were commercially available and used without further purification. Poly(methyl methacrylate) (PMMA, Mn = 30000 g/mol) and Polyvinyl alcohol (PVA) were purchased from Tokyo Chemical Industry (TCI). Methylbenzene was dried by sodium under reflux at 120^{o}C. NMR spectra were recorded on a Bruker Ultra Shield Plus 400MHz with internal standard tetramethylsilane (TMS). Mass spectra were obtained on a Bruker autoflex MALDI-TOF/TOF mass spectrometer. UV-visible absorption spectra were recorded by Shimadzu UV-1750. Photoluminescence spectra were recorded using Hitachi F4600. Differential scanning calorimetry (DSC) was carried out using a Mettler DSC 1 instrument at a scaning rate of 10 Kmin^{-1}. Thermal gravity analysis (TGA) was carried out using a METTLER STARESW 9.30 at a scanning rate of 10 Kmin^{-1} in the atmosphere of nitrogen. Polarizing microscope imaging was captured by an OLYMPUS BX51 (Olympus Optical Co Ltd, Tokyo, Japan) polarizing microscope coupled with a digital camera (Olympus, DP70). SEM was carried out on a Shimadzu SSX-550 device. Single-crystal X-ray analysis was performed on a Bruker Smart Apex CCD diffractometer with graphite monochromated Mo-Ka radiation. X-ray diffraction analysis was carried out on a Rigaku Smartlab (9 kW) X-ray diffractometer using Cu Kα radiation (λ = 1.5406 Å).

Preparation method of S12-BT@PMMA nanocapsules. S12-BT (20 mg), PMMA (200 mg) was dissolved in dichloromethane (4 mL). Then, organic mixture solution was slowly added to 1 wt% PVA water solution (8 mL). The mixed solution was emulsified for 20 minutes (T18 Ultra-Turrax® IKA, 5000 rpm) at room temperature in a borosilicate beaker (50 mL). Successively, the whole emulsion was

transferred into vacuum drying oven with 0.06 MPa for 120 minutes at 40°C. The obtained suspension was centrifuged at 7000 rpm during 15 minutes. Then, a green powder was obtained (163 mg).

Preparation method of the films. Firstly, the dyes (10 mg) were dissolved in hexane (1 ml). Then, the solution of the dyes was drop-casted on the quartz sheets at room temperature. Eventually, when the hexane was completely evaporated, the fluorescent films were formed.

X-ray crystallographic analysis. The single crystal of **S1-BT** was grown from their dichloromethane solution mixed with hexane. Hexane (10 ml) was poured into the solution of **S1-BT** (40 mg) in CH_2Cl_2 (10 ml). The mixture was allowed to settle for a few hours. The precipitate was collected as the green emission crystal.

The calculation method of thermochromic sensitivity (S).

$$S = \frac{\lambda_H - \lambda_R}{T_H - T_R}$$

λ_H : The emission wavelength of the compound at the initial response temperature;

λ_R : The emission wavelength of the compound at the termination response temperature;

T_H : The initial response temperature of the emission color-switching window;

T_R : The termination response temperature of the emission color-switching window.

Theoretical calculations. The calculation was performed using the Gaussian 16 suite of programs. The computational models of **S1-BT** dimers were built from the crystal structure. The optimizations of the complex structures were performed by using a DFT methodology employing the B3LYP functional with 6-31G(d) basis set. Excited state calculations were performed using Time-Dependent DFT (TD-DFT) using the M062X functional, 6-31G(d) basis set. The molecular orbitals were visualized using the Gauss View 5.0 software. The metastable crystal structures of compounds were calculated by using the

Materials Studio software, based on the generation of possible packing arrangements in all reasonable space groups to search for low lying minima in the lattice energy surface.

Photos and videos. The photos and videos were recorded by a Cannon EOS 800D camera.

Synthesis and characterization.

5-ethynyl-1,2,3-trimethoxybenzene,1,2,3-tributoxy-5-ethynylbenzene, 5-ethynyl-1,2,3-tris(octyloxy)benzene,1,2,3-tris(dodecyloxy)-5-ethynylbenzene, 4,4,5,5-tetramethyl-2-(3,4,5-trimethoxyphenyl)-1,3,2-dioxaborolane, 4,4,5,5-tetramethyl-2-(3,4,5-tributoxyphenyl)-1,3,2-dioxaborolane, 4,4,5,5-tetramethyl-2-(3,4,5-tris(octyloxy)phenyl)-1,3,2-dioxaborolane, 4,4,5,5-tetramethyl-2-(3,4,5-tris(dodecyloxy)phenyl)-1,3,2-dioxaborolane were synthesized according to the previously literatures.[1-4] **T12-PH**, **T12-NA**, **T12-CN**, **T1-BT**, **T4-BT**, **T8-BT**, **T12-BT**, **T1-EN**, **T8-EN**, **T12-EN**, **T8-NBT**, **T12-NBT** were synthesized by Sonogashira cross-coupling reaction. **S1-BT**, **S4-BT**, **S8-BT**, **S12-BT**, **S12-EN**, **S4-NBT**, **S12-NBT** were synthesized by Suzuki cross-coupling reaction. All the reactions were carried out under an argon atmosphere using Schlenk technique.

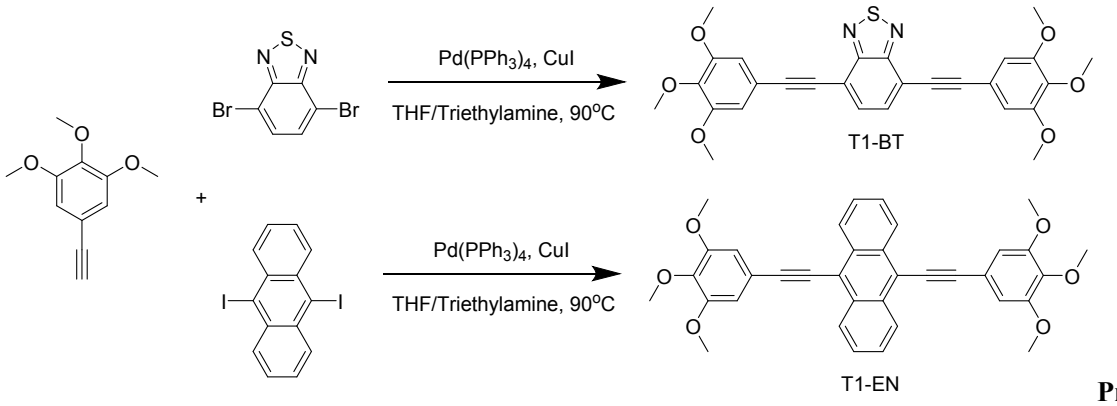

Preparation of T1-BT: A mixture of 5-ethynyl-1,2,3-trimethoxybenzene (2.4 mmol, 460 mg), 4,7-dibromo-2,1,3-benzothiadiazole (1 mmol, 293 mg), $Pd(PPh_3)_4$ (0.06 mmol, 70 mg), CuI (0.12mmol, 23 mg) in degassed triethylamine (5 ml) and 10 ml tetrahydrofuran (THF) was heated under reflux in an argon atmosphere with stirring for 24h. After cooling down to room temperature, the solution was

extracted with ethyl acetate (EA), dried with anhydrous magnesium sulfate, and then purified through the silica gel column chromatography. **T1-BT** was obtained as an orange solid (yield: 79%). ^{1}H NMR (300 MHz, $CDCl_3$, 293 K) δ 7.79 (s, 2H), 6.91 (s, 4H), 3.91(s, 18H). ^{13}C NMR (126 MHz, $CDCl_3$, 293 K) δ 154.38, 153.21, 139.76, 132.37, 117.41, 117.10, 109.38, 97.74, 84.49, 61.00, 56.28. MALDITOF-MS m/z: Calculated: 516.136, found: 516.197.

Preparation of T1-EN: Following the general procedure for the synthesis of **T1-BT**, **T1-EN** was obtained as an orange solid (yield: 82%).^{1}H NMR (500 MHz, $CDCl_3$, 293 K) δ 8.69 (dd, J = 6.6, 3.2 Hz, 4H), 7.66 (dd, J = 6.7, 3.2 Hz, 4H), 7.00 (s, 4H), 3.98 (s, 12H), 3.94 (s, 6H).^{13}C NMR (101 MHz, $CDCl_3$, 293 K) δ 153.33, 139.32, 132.11, 127.28, 126.86, 118.41, 118.38, 108.93, 102.49, 85.55, 61.12, 56.36. MALDITOF-MS m/z: Calculated: 558.202, found: 558.246.

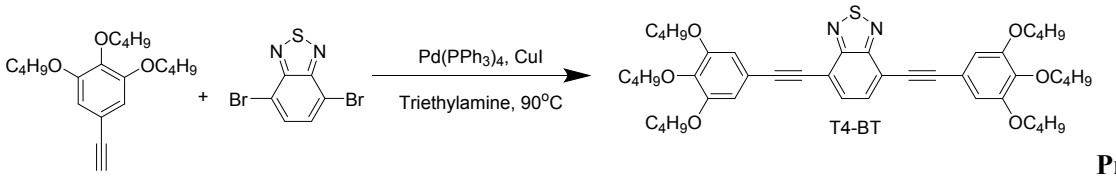

Preparation of T4-BT: Following the general procedure for the synthesis of **T1-BT**, **T4-BT** was obtained as a yellow solid (yield: 76%). ^{1}H NMR (300 MHz, $CDCl_3$, 293 K) δ 7.75 (s, 2H), 6.87 (s, 4H), 4.02 (m, 12H), 1.79 (m, 12H), 1.63 – 1.38 (m, 12H), 0.98 (m, 18H). ^{13}C NMR (101 MHz, $CDCl_3$, 293 K) δ 154.38, 153.09, 139.76, 132.38, 117.08, 116.85, 110.48, 98.08, 84.20, 73.21, 68.89, 32.34, 31.38, 19.28, 19.19, 13.93, 13.87. MALDITOF-MS m/z: Calculated: 768.417, found: 768.448.

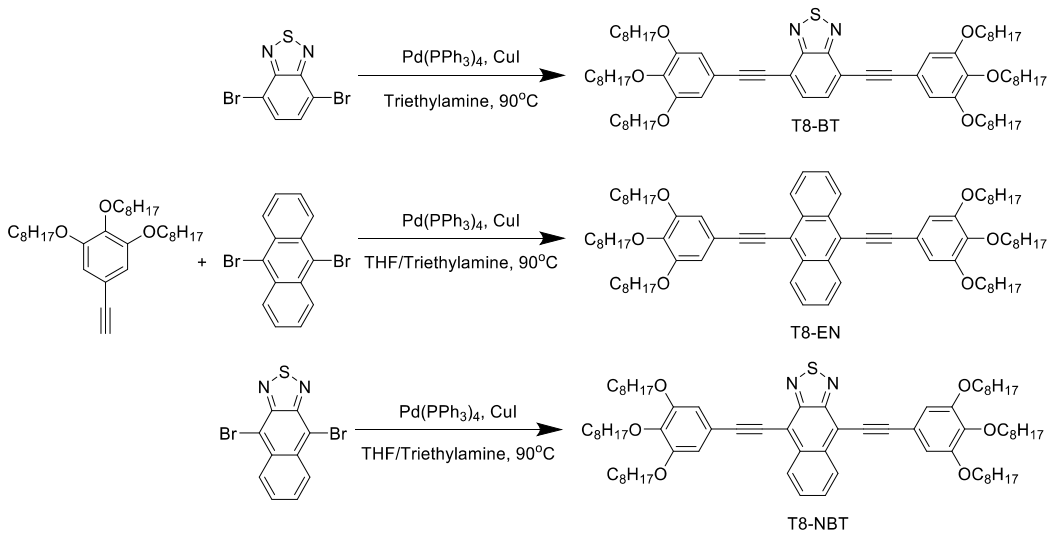

Preparation of T8-BT: Following the general procedure for the synthesis of **T1-BT**, **T8-BT** was obtained as a yellow solid (yield: 62%). ^{1}H NMR (500 MHz, $CDCl_3$, 293 K) δ 7.76 (s, 2H), 6.86 (s, 4H), 4.01 (m, 12H), 1.79 (m, 12H), 1.58 – 1.06 (m, 60H), 0.89 (m, 18H). ^{13}C NMR (101 MHz, $CDCl_3$, 293 K) δ 154.39, 153.08, 139.77, 132.37, 117.09, 116.83, 110.48, 98.11, 84.18, 73.61, 69.21, 31.93, 31.86, 30.35, 29.56, 29.38, 29.32, 26.10, 22.73, 22.70, 14.14. MALDITOF-MS m/z: Calculated: 1104.793, found: 1104.846.

Preparation of T8-EN: Following the general procedure for the synthesis of **T1-BT**, **T8-EN** was obtained as a green solid (yield: 80%). ^{1}H NMR (500 MHz, $CDCl_3$, 293 K) δ 8.67 (dd, J = 6.6, 3.2 Hz, 4H), 7.64 (dd, J = 6.6, 3.2 Hz, 4H), 6.95 (s, 4H), 4.06 (m, 12H), 1.82 (m, 12H), 1.51 (m, 12H), 1.43 – 1.19 (m, 48H), 0.89 (m, 18H).^{13}C NMR (101 MHz, $CDCl_3$, 293 K) δ 153.25, 139.57, 132.12, 127.34, 126.76, 118.44, 117.83, 110.29, 102.81, 85.20, 73.69, 69.34, 31.96, 31.88, 30.39, 29.60, 29.43, 29.35, 26.16, 22.76, 22.73, 14.16. MALDITOF-MS m/z: Calculated: 1146.862, found: 1146.946.

Preparation of T8-NBT: Following the general procedure for the synthesis of **T1-BT**, **T8-NBT** was obtained as a dark solid (yield: 52%). ^{1}H NMR (400 MHz, $CDCl_3$, 293 K) δ 8.60 (dd, J = 6.8, 3.2 Hz, 2H), 7.61 (dd, J = 6.7, 3.1 Hz, 2H), 6.97 (s, 4H), 4.04 (m, 12H), 1.80 (m, 12H), 1.71 – 1.10 (m, 60H), 1.06 – 0.78 (m, 18H). ^{13}C NMR (101 MHz, $CDCl_3$, 293 K) δ 153.18, 152.71, 139.94, 134.70, 127.86, 127.68, 117.23, 112.56, 110.56, 104.78, 84.07, 73.67, 69.31, 31.95, 31.87, 30.37, 29.58, 29.41, 29.34, 26.13, 22.74, 22.71, 14.14. MALDITOF-MS m/z: Calculated: 1154.809, found: 1154.674.

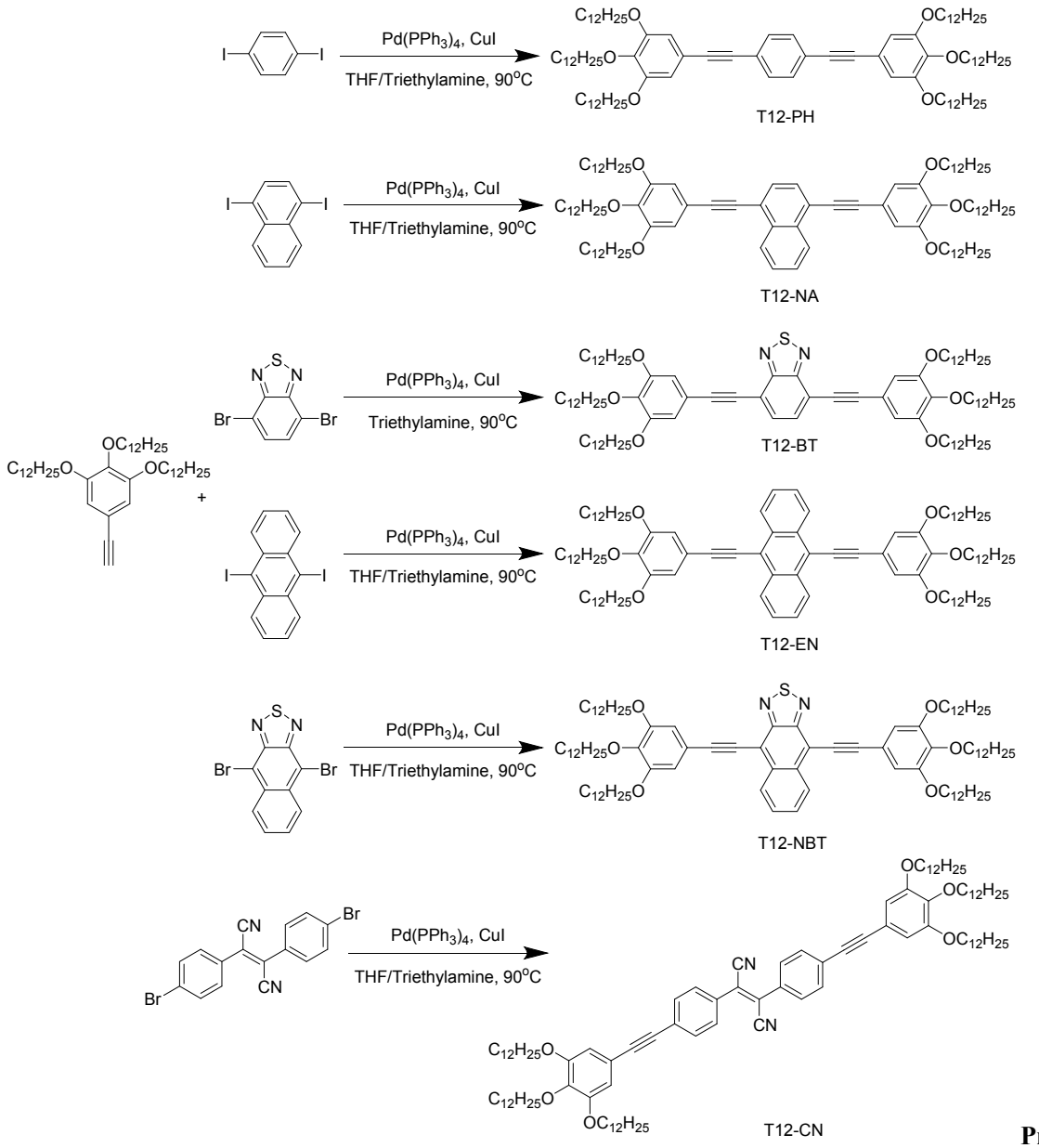

Preparation of T12-BT: Following the general procedure for the synthesis of **T1-BT**, **T12-BT** was obtained as a green solid (yield: 72%).^{1}H NMR (300 MHz, $CDCl_3$, 293 K) δ 7.76 (s, 2H), 6.86 (s, 4H), 4.01 (m, 12H), 1.84 (m, 12H), 1.47 (m, 12H)1.28 (m, 96H), 0.88 (m, 18H). ^{13}C NMR (101 MHz, $CDCl_3$, 293 K) δ 154.39, 153.08, 139.77, 132.37, 117.10, 116.83, 110.49, 98.11, 84.18, 73.61, 69.21, 31.98, 31.96, 30.35, 29.78, 29.74, 29.68, 29.63, 29.43, 29.40, 29.35, 26.11, 22.73, 14.16. MALDITOF-MS m/z: Calculated: 1442.174, found: 1442.222.

Preparation of T12-PH: Following the general procedure for the synthesis of **T1-BT**, **T12-PH** was

obtained as a white solid (yield: 85%). ^{1}H NMR (300 MHz, $CDCl_3$, 293 K) δ 7.47 (s, 4H), 6.73 (s, 4H), 3.98 (m, 12H), 1.93 – 1.63 (m, 12H), 1.51 (m, 12H), 1.27 (s, 96H), 0.88 (m, 18H). ^{13}C NMR (101 MHz, $CDCl_3$, 293 K) δ 153.03, 139.21, 131.44, 123.02, 117.39, 110.08, 91.66, 87.88, 73.58, 69.13, 31.96, 30.34, 29.79, 29.77, 29.74, 29.70, 29.68, 29.63, 29.43, 29.41, 29.35, 26.11, 22.74, 14.16. MALDITOF-MS m/z: Calculated: 1384.209, found: 1383.181.

Preparation of T12-NA: Following the general procedure for the synthesis of **T1-BT**, **T12-NA** was obtained as a light green solid (yield: 79%). ^{1}H NMR (300 MHz, $CDCl_3$, 293 K) δ 8.44 (dd, J = 6.3, 3.3 Hz, 2H), 7.70 (s, 2H), 7.63 (dd, J = 6.3, 3.3 Hz, 2H), 6.84 (s, 4H), 4.02 (m, 12H), 1.95 – 1.64 (m, 21H), 1.49 (s, 12H), 1.27 (s, 96H), 0.88 (m, 18H). ^{13}C NMR (101 MHz, $CDCl_3$, 293 K) δ 153.13, 139.38, 133.06, 129.65, 127.18, 126.71, 121.47, 117.58, 110.22, 96.38, 86.27, 73.63, 69.23, 31.97, 30.37, 29.80, 29.78, 29.75, 29.70, 29.65, 29.45, 29.41, 29.39, 26.14, 22.74, 14.16. MALDITOF-MS m/z: Calculated: 1434.225, found: 1434.524.

Preparation of T12-CN: Following the general procedure for the synthesis of **T1-BT**, **T12-CN** was obtained as a yellow solid (yield: 67%). ^{1}H NMR (500 MHz, $CDCl_3$, 293 K) δ 7.84 (d, J = 8.2 Hz, 4H), 7.65 (d, J = 8.2 Hz, 4H), 6.76 (s, 4H), 4.00 (m, 12H), 1.85 – 1.70 (m, 12H), 1.48 (m, 12H), 1.27 (s, 96H), 0.88 (m, 18H). ^{13}C NMR (101 MHz, $CDCl_3$, 293 K) δ 153.10, 139.63, 132.15, 131.16, 129.46, 128.76, 127.34, 124.39, 116.83, 116.54, 110.27, 93.75, 87.19, 73.61, 69.17, 31.99, 31.96, 30.35, 29.79, 29.74, 29.70, 29.68, 29.63, 29.44, 29.41, 29.35, 26.12, 22.74, 14.16. MALDITOF-MS m/z: Calculated: 1536.246, found: 1536.065.

Preparation of T12-EN: Following the general procedure for the synthesis of **T1-BT**, **T12-EN** was obtained as a green solid (yield: 67%). ^{1}H NMR (300 MHz, $CDCl_3$, 293 K) δ 8.71 (dd, J = 6.6, 3.2 Hz, 4H), 7.67 (dd, J = 6.6, 3.2 Hz, 4H), 7.00 (s, 4H), 4.30 – 3.88 (m, 12H), 1.87 (m, 12H), 1.54 (s, 12H), 1.32 (s, 96H), 0.92 (m, 18H). ^{13}C NMR (101 MHz, $CDCl_3$, 293 K) δ 153.24, 139.57, 132.12, 127.34, 126.75, 118.44, 117.84, 110.28, 102.80, 85.20, 73.69, 69.33, 31.99, 31.97, 30.40, 29.82, 29.80, 29.76, 29.71, 29.67, 29.47, 29.45, 29.42, 26.17, 22.74, 14.17. MALDITOF-MS m/z: Calculated: 1484.241, found: 1484.462.

Preparation of T12-NBT: Following the general procedure for the synthesis of **T1-BT**, **T12-NBT** was

obtained as a dark solid (yield: 67%). ^{1}H NMR (300 MHz, $CDCl_3$, 293 K) δ 8.62 (s, 2H), 7.62 (s, 2H), 7.00 (s, 4H), 4.07 (m, 12H), 1.84 (m, 12H), 1.34 (m, 108H), 0.90 (m, 18H). ^{13}C NMR (101 MHz, $CDCl_3$, 293 K) δ 153.19, 152.73, 139.96, 134.72, 127.86, 127.70, 117.22, 112.58, 110.58, 104.79, 84.05, 73.67, 69.32, 31.96, 30.38, 29.80, 29.75, 29.70, 29.65, 29.45, 29.41, 26.14, 22.73, 14.16. MALDITOF-MS m/z: Calculated: 1492.187, found: 1492.159.

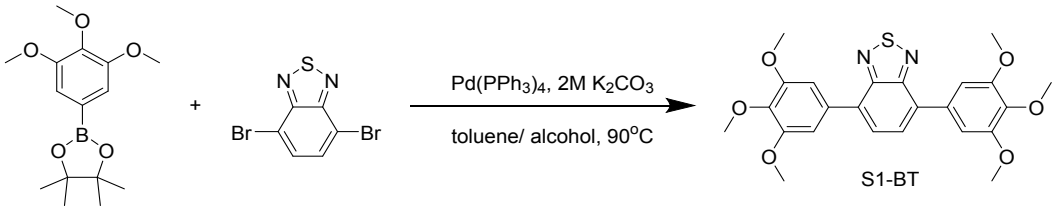

Preparation of S1-BT: 4,4,5,5-tetramethyl-2-(3,4,5-trimethoxyphenyl)-1,3,2-dioxaborolane (2.4 mmol, 706 mg), 4,7-dibromo-2,1,3-benzothiadiazole (1 mmol, 293 mg), $Pd(PPh_3)_4$ (0.04 mmol, 46 mg) were dissolved in degassed toluene (6 ml). 2M K_2CO_3 (3 ml) and alcohol (3 ml) were added to the above solution. The mixture was heated under reflux in an argon atmosphere with stirring for 24 h. After cooling down to room temperature, the solution was extracted with ethyl acetate (EA), dried with anhydrous magnesium sulfate, and then purified through the silica gel column chromatography. **S1-BT** was obtained as a green solid (yield: 86%). ^{1}H NMR (300 MHz, $CDCl_3$, 293 K) δ 7.77 (s, 2H), 7.24 (d, J = 13.4 Hz, 4H), 3.96 (d, J = 6.4 Hz, 18H). ^{13}C NMR (101 MHz, $CDCl_3$, 293 K) δ 154.04, 153.32, 138.43, 133.13, 132.90, 127.84, 106.63, 61.00, 56.30. MALDITOF-MS m/z: Calculated: 468.136, found: 468.092.

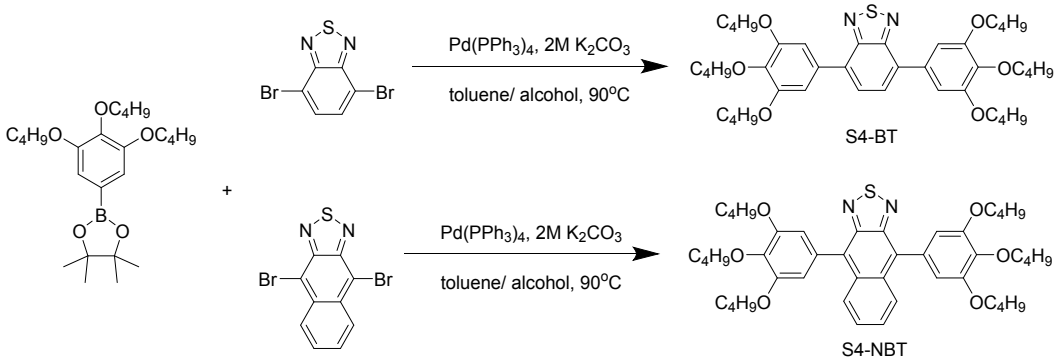

Preparation of S4-BT: Following the general procedure for the synthesis of **S1-BT**, **S4-BT** was obtained as a green solid (yield: 65%). ^{1}H NMR (500 MHz, $CDCl_3$, 293 K) δ 7.73 (s, 2H), 7.19 (s, 4H), 4.08 (m,

12H), 1.81 (m, 12H), 1.55 (m, 12H), 0.99 (t, J = 7.4 Hz, 18H).^{13}C NMR (126 MHz, $CDCl_3$, 293 K) δ 154.14, 153.23, 138.97, 133.10, 132.36, 127.70, 108.34, 69.08, 32.44, 31.55, 19.34, 19.26, 13.94, 13.88.MALDITOF-MS m/z: Calculated: 720.417, found: 720.362.

Preparation of S4-NBT: Following the general procedure for the synthesis of **S1-BT**, **S4-NBT** was obtained as a red solid (yield: 65%). ^{1}H NMR (500 MHz, $CDCl_3$, 293 K) δ 8.03 (dd, J = 7.0, 3.2 Hz, 2H), 7.35 (dd, J = 7.1, 3.2 Hz, 2H), 6.81 (s, 4H), 4.07 (m, 12H), 1.81 (m, 12H), 1.66 – 1.43 (m, 12H), 0.99 (m, 18H). ^{13}C NMR (101 MHz, $CDCl_3$, 293 K) δ 153.12, 151.26, 138.14, 132.08, 131.32, 130.42, 127.24, 126.31, 109.75, 73.22, 68.84, 32.50, 31.49, 19.33, 19.30, 14.03, 13.92. MALDITOF-MS m/z: Calculated: 770.432, found: 770.410.

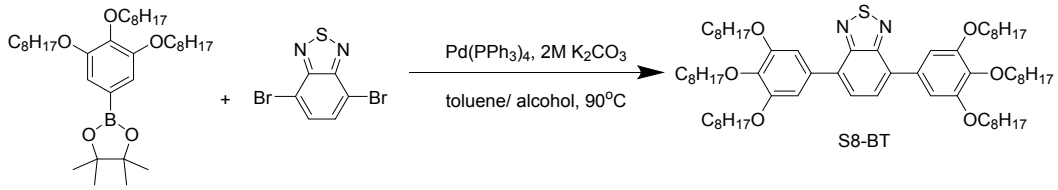

Preparation of S8-BT: Following the general procedure for the synthesis of **S1-BT**, **S8-BT** was obtained as a green solid (yield: 87%). ^{1}H NMR (300 MHz, $CDCl_3$, 293 K) δ 7.73 (s, 2H), 7.18 (s, 4H), 4.07 (m, 12H), 1.83 (m, 12H), 1.43 (m, 60H), 1.10 – 0.60 (m, 18H). ^{13}C NMR (101 MHz, $CDCl_3$, 293 K) δ 154.11, 153.19, 138.76, 133.08, 132.38, 127.74, 108.11, 73.62, 69.29, 31.98, 31.89, 30.44, 29.63, 29.48, 29.46, 29.37, 26.19, 22.76, 22.73, 14.15. MALDITOF-MS m/z: Calculated: 1056.793, found: 1056.764.

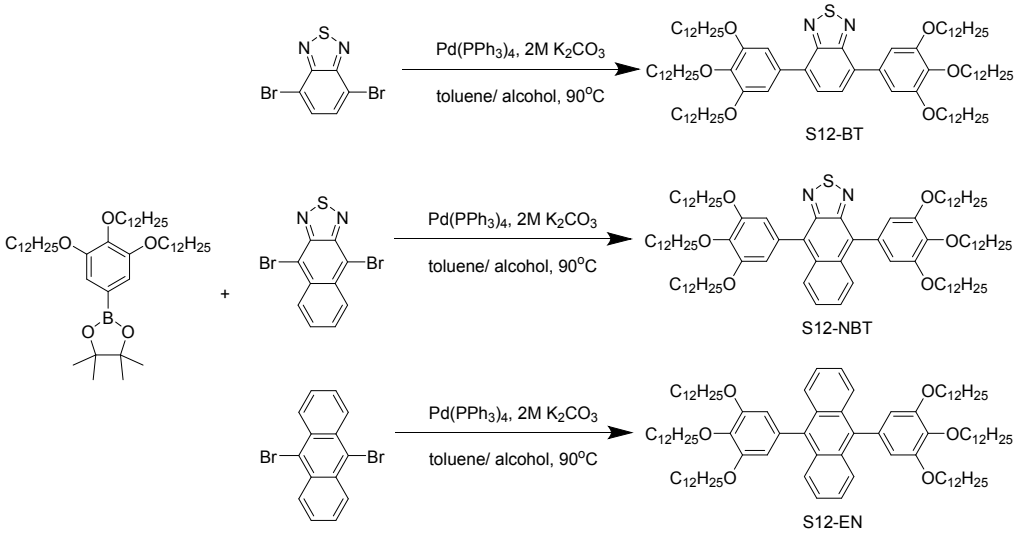

Preparation of S12-BT: Following the general procedure for the synthesis of **S1-BT**, **S12-BT** was obtained as a green solid (yield: 75%). ^{1}H NMR (300 MHz, Chloroform-d) δ 7.73 (s, 2H), 7.18 (s, 4H), 4.06 (m, 12H), 1.99 – 1.68 (m, 12H), 1.51 (d, *J* = 7.2 Hz, 12H), 1.27 (s, 96H), 0.88 (m, 18H). ^{13}C NMR (101 MHz, $CDCl_3$, 293 K) δ 154.09, 153.16, 138.69, 133.08, 132.38, 127.74, 108.09, 73.64, 69.29, 58.45, 50.81, 31.97, 31.95, 30.41, 29.80, 29.73, 29.69, 29.48, 29.46, 29.44, 29.39, 26.17, 22.71, 18.41, 14.14. MALDITOF-MS m/z: Calculated: 1393.168, found: 1393.237.

Preparation of S12-NBT: Following the general procedure for the synthesis of **S1-BT**, **S12-NBT** was obtained as a red solid (yield: 53%).^{1}H NMR (300 MHz, $CDCl_3$, 293 K) δ 8.06 (d, *J* = 10.4 Hz, 2H), 7.49 – 7.33 (m, 2H), 6.85 (s, 4H), 4.09 (m, 12H), 1.86 (m, 12H), 1.69 – 1.25 (m, 108H), 0.92 (m, 18H). ^{13}C NMR (101 MHz, $CDCl_3$, 293 K) δ 153.11, 151.26, 138.18, 132.08, 131.28, 130.42, 127.24, 126.29, 109.77, 73.60, 69.15, 31.99, 31.95, 30.52, 29.85, 29.82, 29.76, 29.72, 29.68, 29.48, 29.45, 29.39, 26.23, 26.15, 22.75, 22.72, 14.15. MALDITOF-MS m/z: Calculated: 1444.187, found: 1444.250.

Preparation of S12-EN: Following the general procedure for the synthesis of **S1-BT**, **S12-EN** was obtained as a green solid (yield: 88%).^{1}H NMR (300 MHz, $CDCl_3$, 293 K) δ 7.78 (dd, *J* = 6.8, 3.2 Hz, 4H), 7.35 (dd, *J* = 6.8, 3.1 Hz, 4H), 6.65 (s, 4H), 4.04 (m, 12H), 1.82 (m, 12H), 1.45 – 1.22 (m, 108H), 0.87 (m, 18H). ^{13}C NMR (75 MHz, $CDCl_3$, 293 K) δ 153.08, 137.30, 133.88, 129.82, 127.06, 124.99, 109.95, 73.58, 69.23, 31.91, 31.43, 30.51, 30.22, 29.68, 29.34, 26.25, 26.11, 22.67. MALDITOF-MS m/z: Calculated: 1436.241, found: 1436.247.

Supplementary Figures

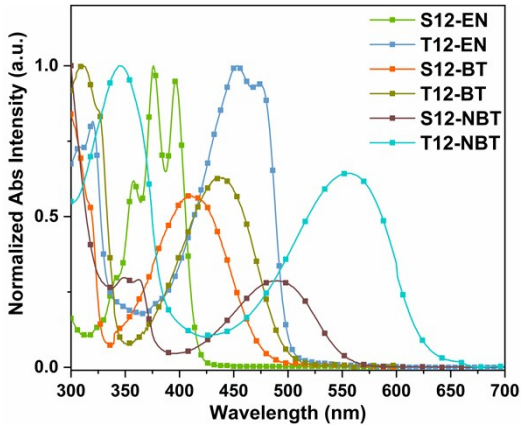

Supplementary Figure 1. Normalized absorption spectra of **S12-EN**, **T12-EN**, **S12-BT**, **T12-BT**, **S12-NBT** and **T12-NBT** in dichloromethane (10^{-5} M).

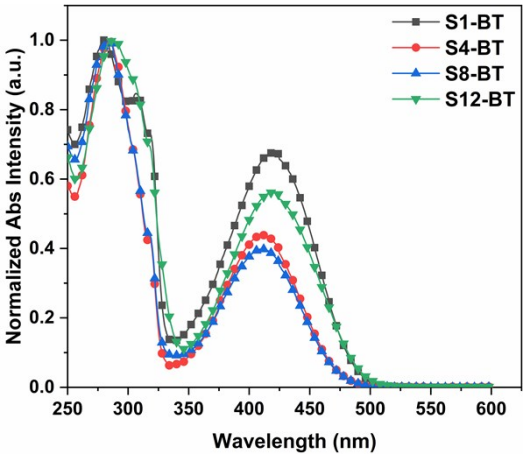

Supplementary Figure 2. Normalized absorption spectra of **S1-BT**, **S4-BT**, **S8-BT** and **S12-BT** in DCM (10^{-5} M).

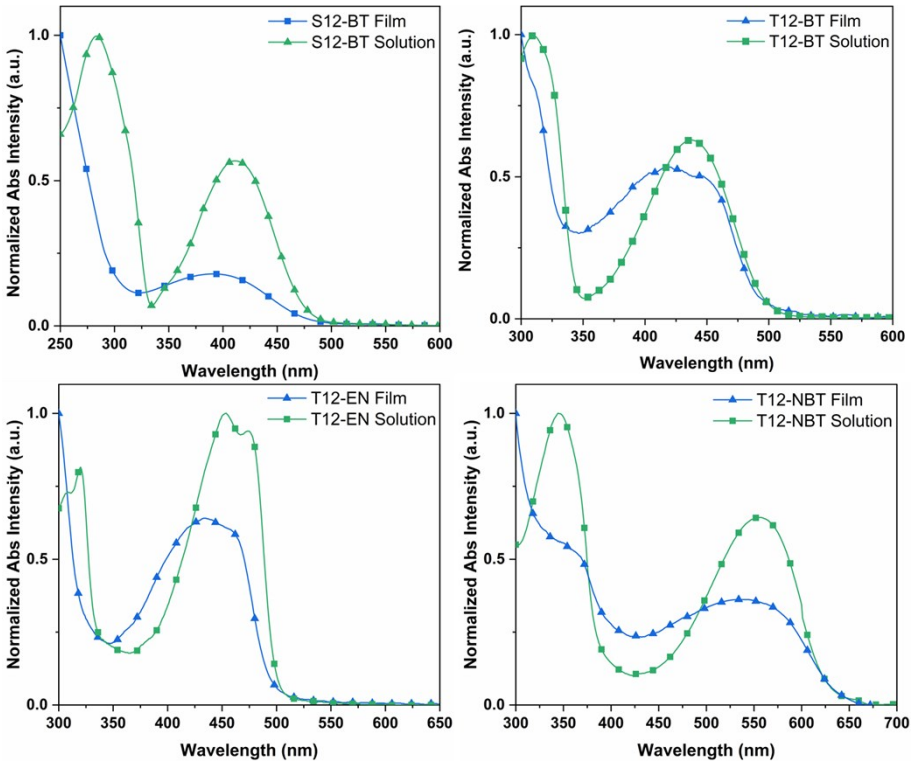

Supplementary Figure 3. Normalized absorption spectra of **S12-BT**, **T12-BT**, **T12-EN** and **T12-NBT** in DCM (10^{-5} M) and films.

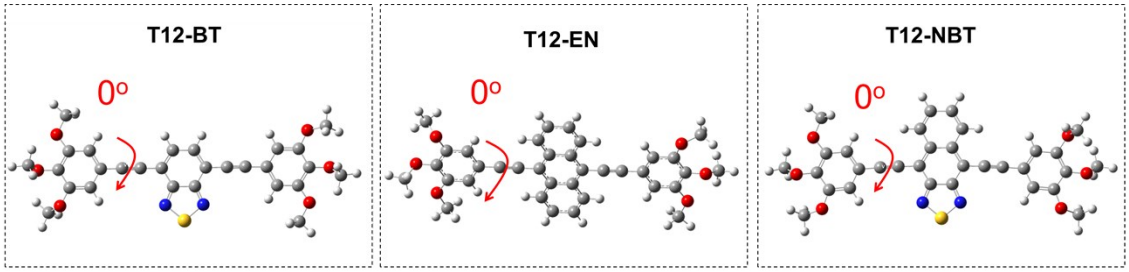

Supplementary Figure 4. Torsion angles of **T12-BT**, **T12-EN** and **T12-NBT** in the optimized ground state geometry (DFT calculations at the B3LYP/6-31G(d) level).

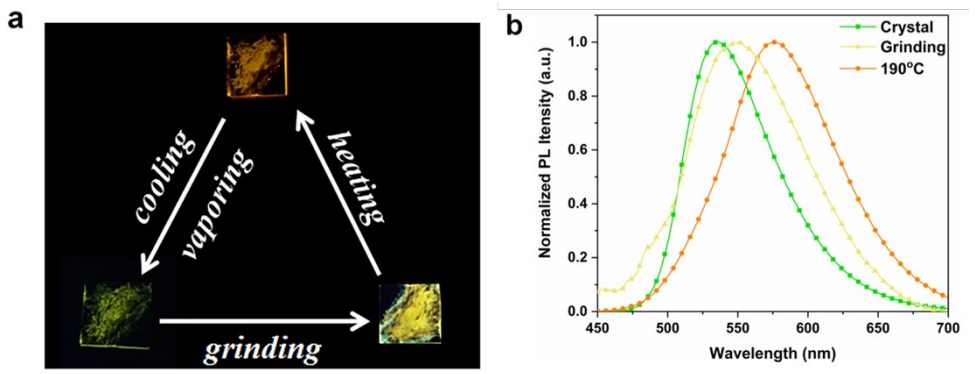

Supplementary Figure 5. (a) Digital images of **S1-BT** samples recorded under UV light (quartz sheet size: 1 cm * 1 cm). **(b)** Normalized PL spectra of **S1-BT** solid sample during grinding and heating.

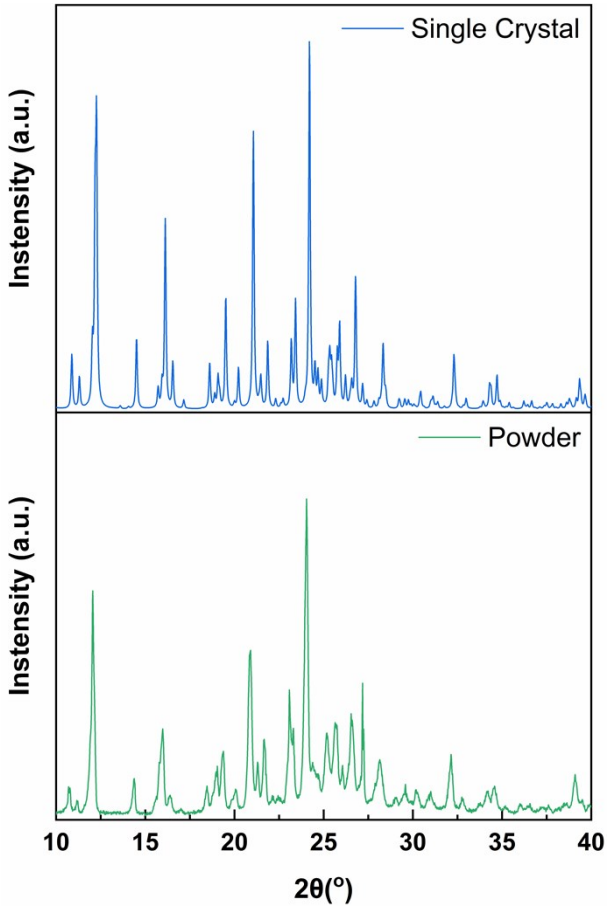

Supplementary Figure 6. XRD pattern of **S1-BT** at room temperature.

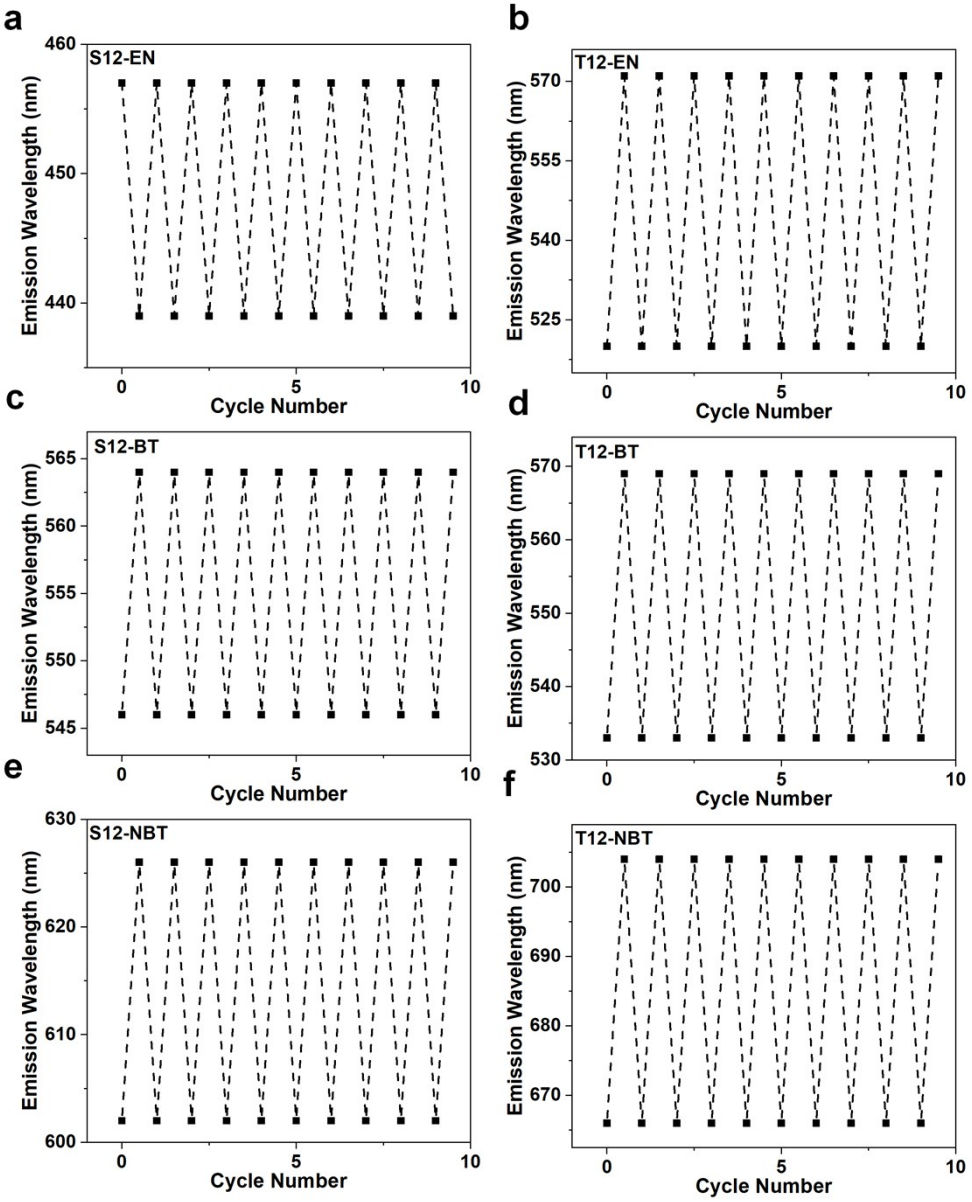

Supplementary Figure 7. Plots of emission wavelength of **S12-EN**, **T12-EN**, **S12-BT**, **T12-BT**, **S12-NBT**, **T12-NBT** during heating–cooling cycles.

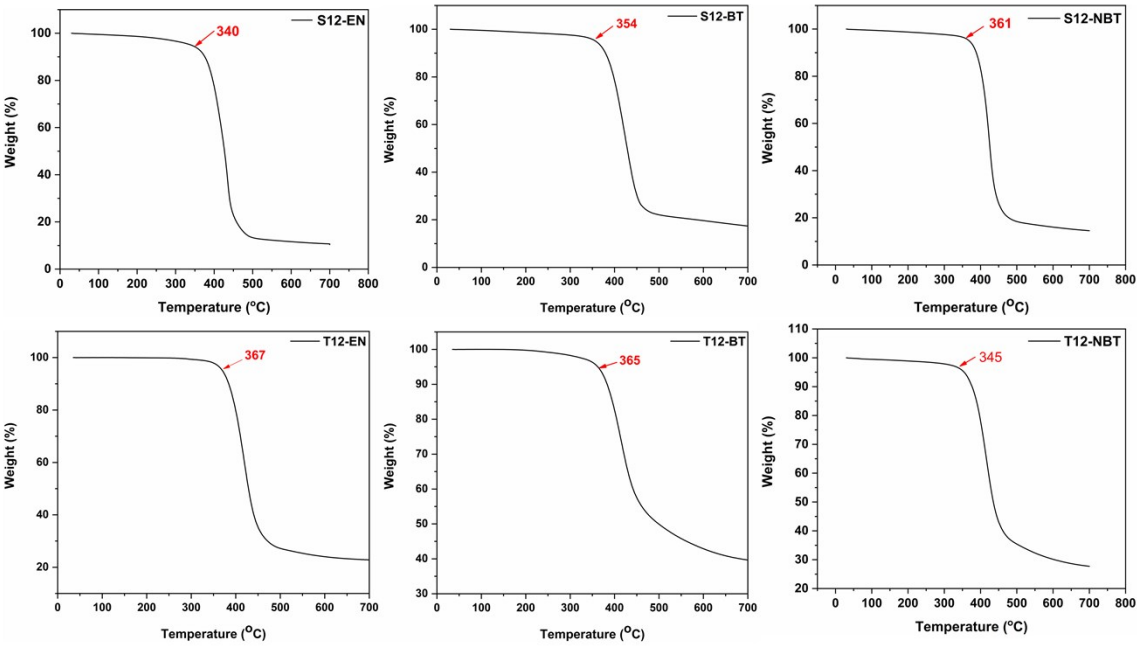

Supplementary Figure 8. TGA curves of **S12-EN**, **T12-EN**, **S12-BT**, **T12-BT**, **S12-NBT**, **T12-NBT**.

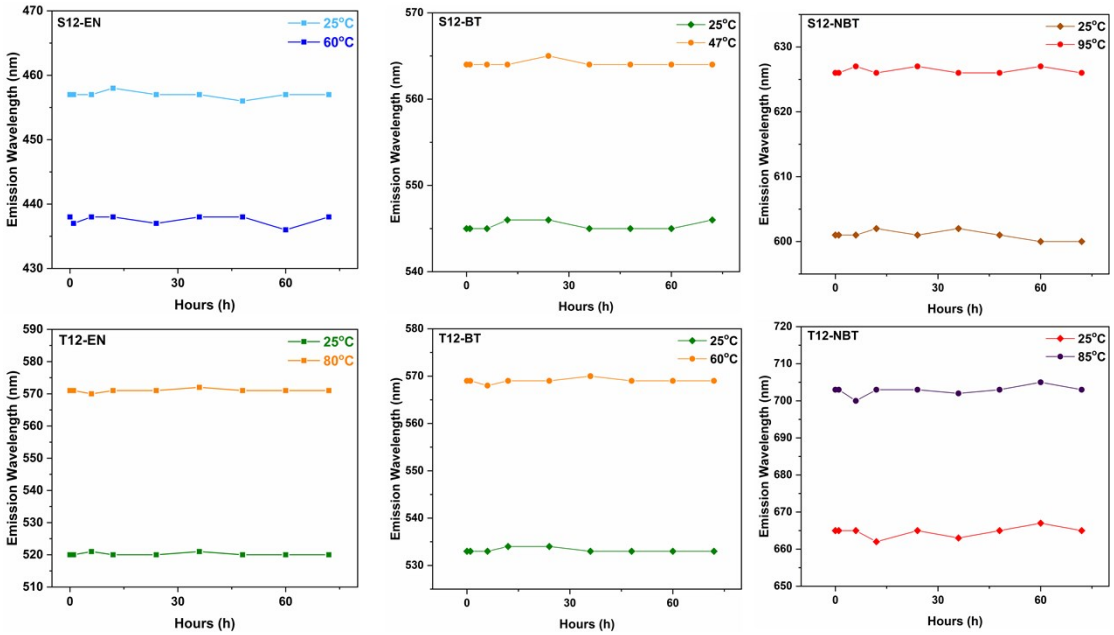

Supplementary Figure 9. Emission stability of **S12-EN**, **T12-EN**, **S12-BT**, **T12-BT**, **S12-NBT**, **T12-NBT** at room temperature and high temperature.

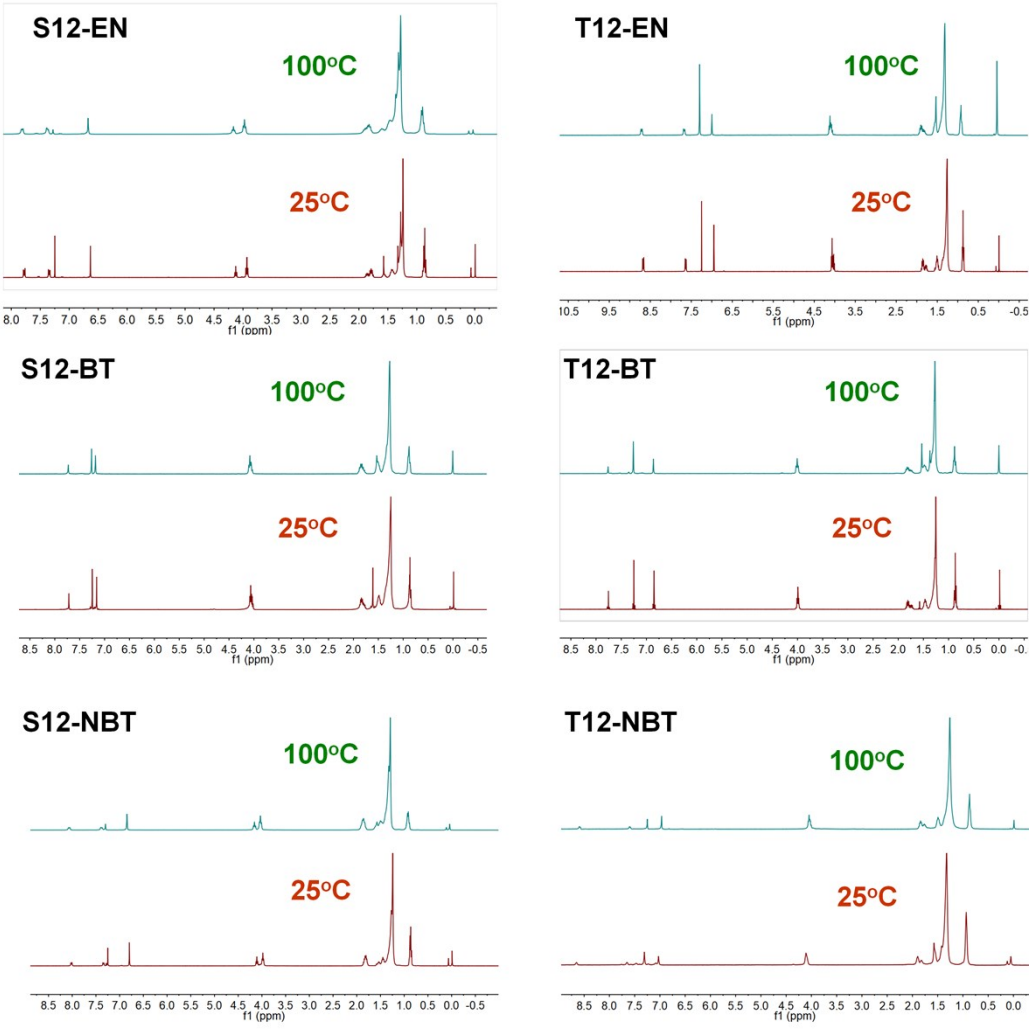

Supplementary Figure 10. Variable temperature ^{1}H NMR spectra of **S12-EN**, **T12-EN**, **S12-BT**, **T12-BT**, **S12-NBT**, **T12-NBT**.

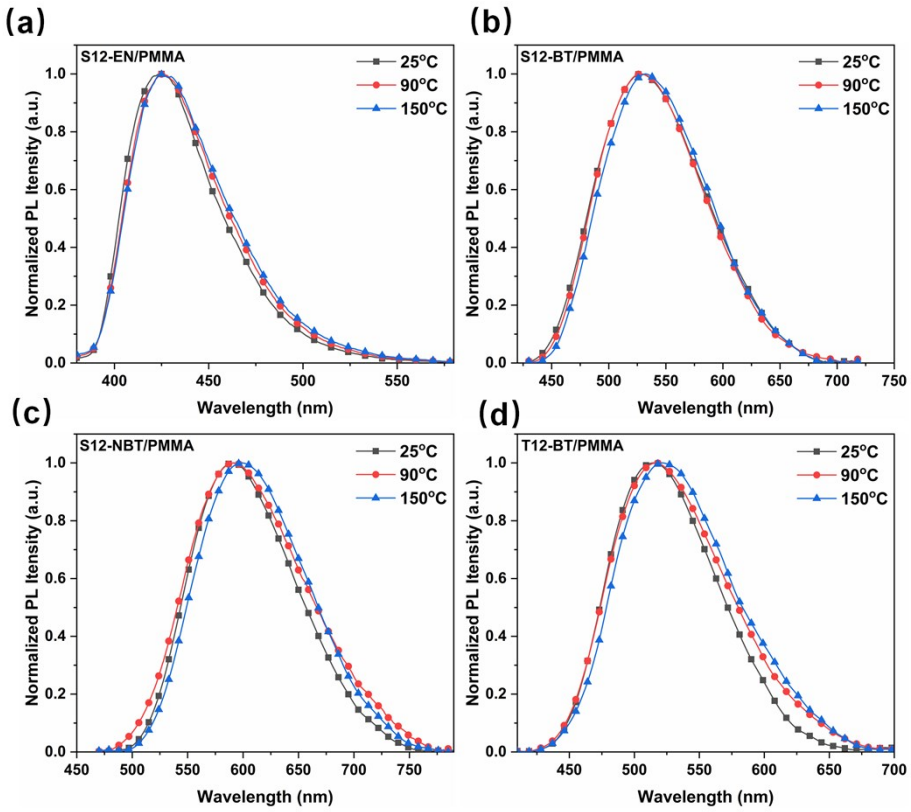

Supplementary Figure 11. Normalized PL spectra of **S12-EN (a)**, **S12-BT (b)**, **S12-NBT (c)** and **T12-BT (d)** dispersed in PMMA (0.1 wt%).

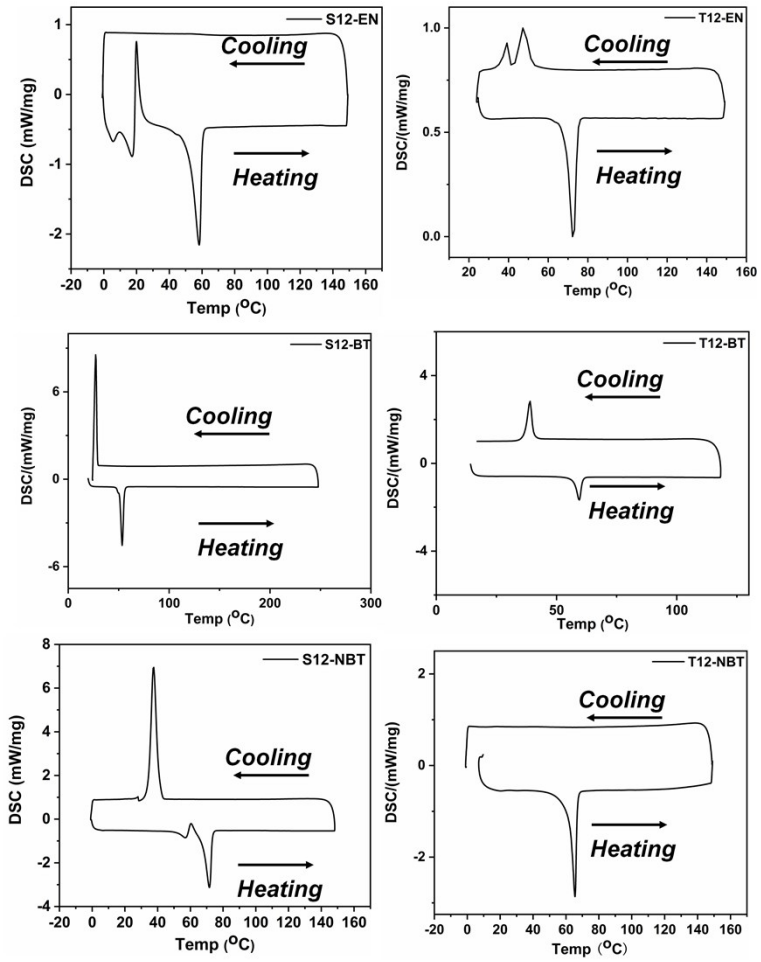

Supplementary Figure 12. DSC curves of **S12-BT**, **T12-BT**, **S12-EN**, **T12-EN**, **S12-NBT** and **T12-NBT**.

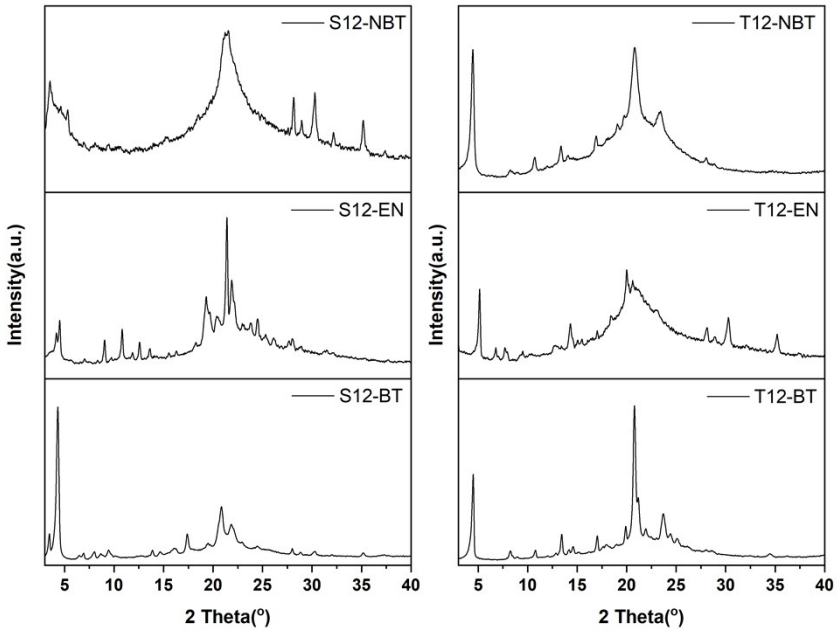

Supplementary Figure 13. XRD pattern of **S12-EN**, **T12-EN**, **S12-BT**, **T12-BT**, **S12-NBT**, **T12-NBT** at room temperature.

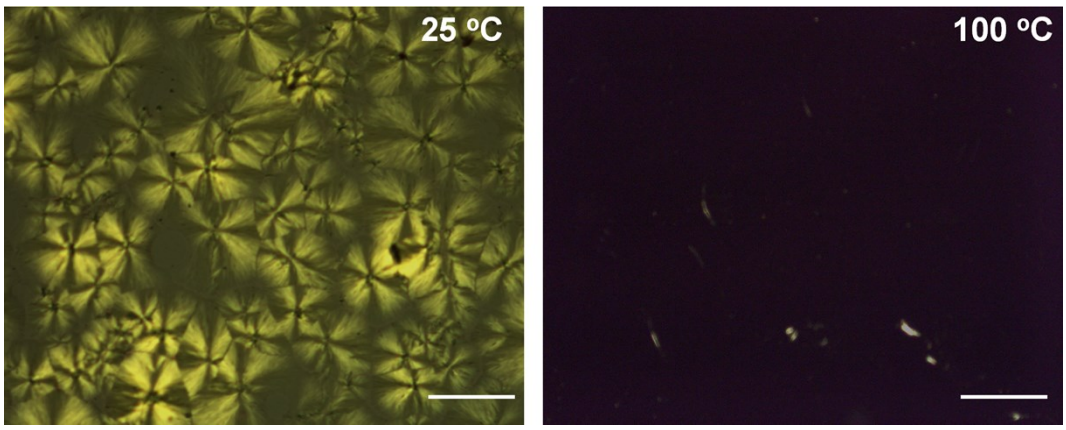

Supplementary Figure 14. Polarizing optical microscope of **S12-BT** at 25°C and 100°C (scale bar: 200 μm).

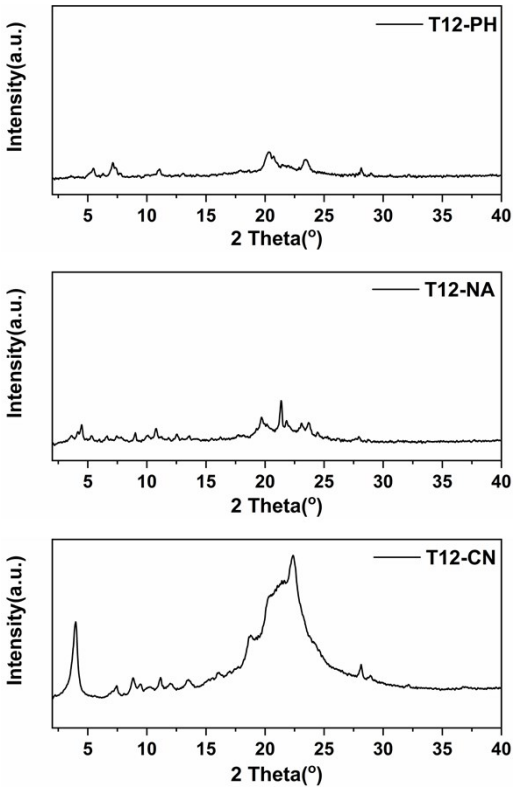

Supplementary Figure 15. XRD pattern of **T12-PH**, **T12-NA**, **T12-CN** at room temperature.

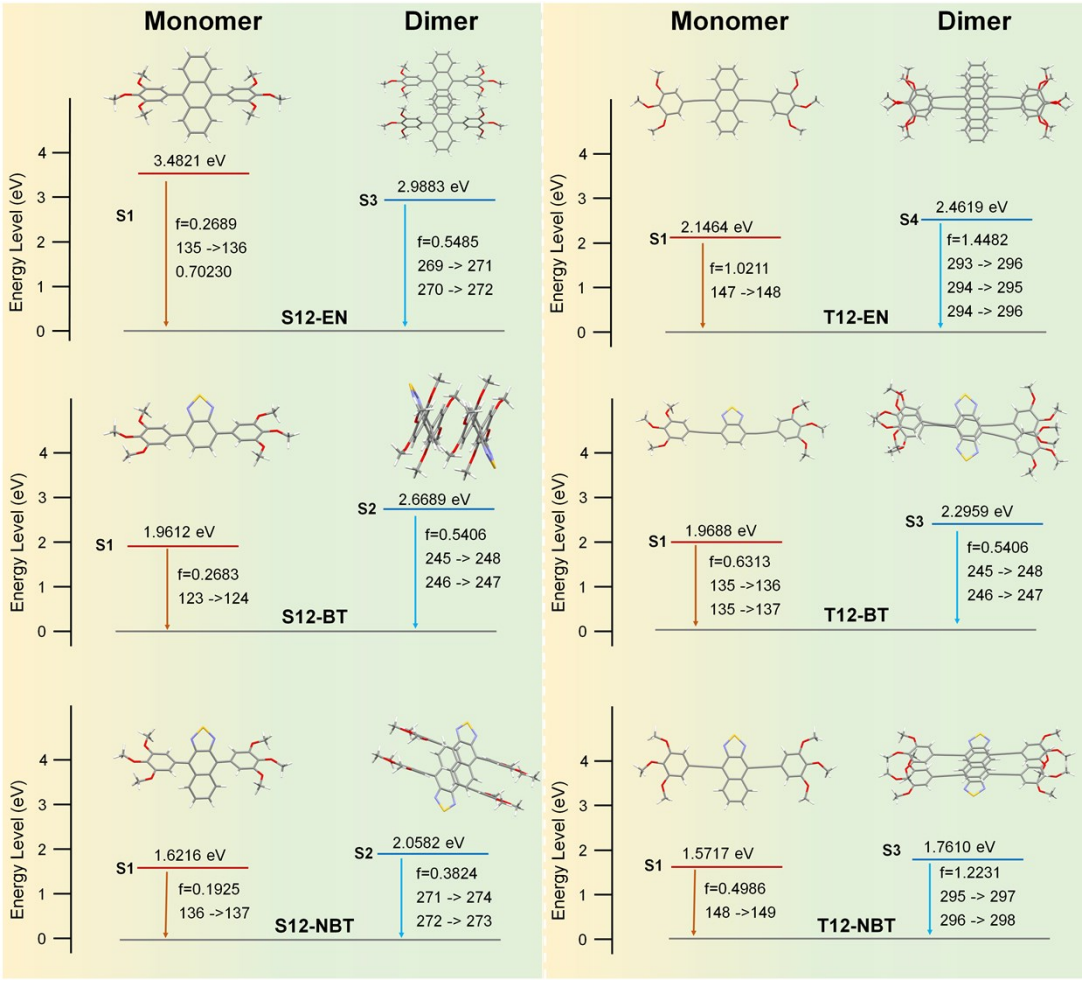

Supplementary Figure 16. TD-DFT transitions for dimer and monomer of **S12-EN**, **T12-EN**, **S12-BT**, **T12-BT**, **S12-NBT**, **T12-NBT** at room temperature.

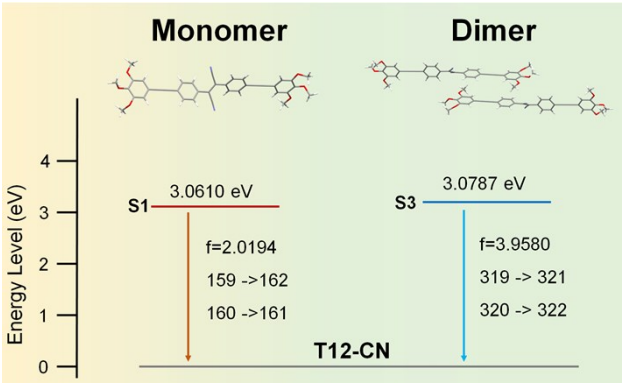

Supplementary Figure 17. TD-DFT transitions for dimer and monomer of **T12-CN** at room temperature.

The poor crystallinity of these materials from the long alky chain hinders us to obtain the dimer of single-crystal data. Hence, to obtain the dimer structure, the metastable crystal structures of these compounds were calculated by using the Materials Studio software, based on the generation of possible packing arrangements in all reasonable space groups to search for low lying minima in the lattice energy surface. Firstly, the molecular structure was optimized by Gaussian 16 in the ground state. Then the energy calculations were performed using Polymorph modules to provide possible crystal data in Figure S25-31. In order to improve the accuracy of theoretical calculations, we extracted the optimal dimer structure from predicted crystal data.[5] As a result, in the predicted S1-BT dimer, two adjacent molecules are stacked in the forms of an H-aggregated state based on π−π interactions with an intermolecular distance of 3.8 Å. In addition, C–H···O or C–H···S interactions also were not be found in the crystal, and the intermolecular torsional angles along the D-A-D conjugated skeleton were approximately 38°, which is well consistent with S1-BT dimer of single crystal. Similarly, the predicted dimer of T12-BT, T12-EN, S12-NBT and T12-NBT display H-type aggregation with opposite vertical dipole direction in the acceptor groups of the dimers. However, the predicted S12-EN dimer show excimer packing mode with antiparallel anthracene plane led to PL spectral blueshift during heating. In contrast with S12-EN, T12-CN shows aggregation without vertical dipole. To get a deeper insight into the proposed mechanism, the packing mode, energy level and oscillator strength of these dimers were calculated by time-dependent density functional theory (TD-DFT) using the M062X density functional in Figure S16 and Figure S17. The overall calculated results successfully reproduce the experimentally observed luminescence trends for all compounds. Therefore, we can ensure that suitable intermolecular interactions and the strength of the vertical dipole of the acceptor moiety determine the thermochromic luminescence phenomenon. It is worth mentioning that no obvious aggregation of T12-PH and T12-NA could be observed

from the POM and XRD.

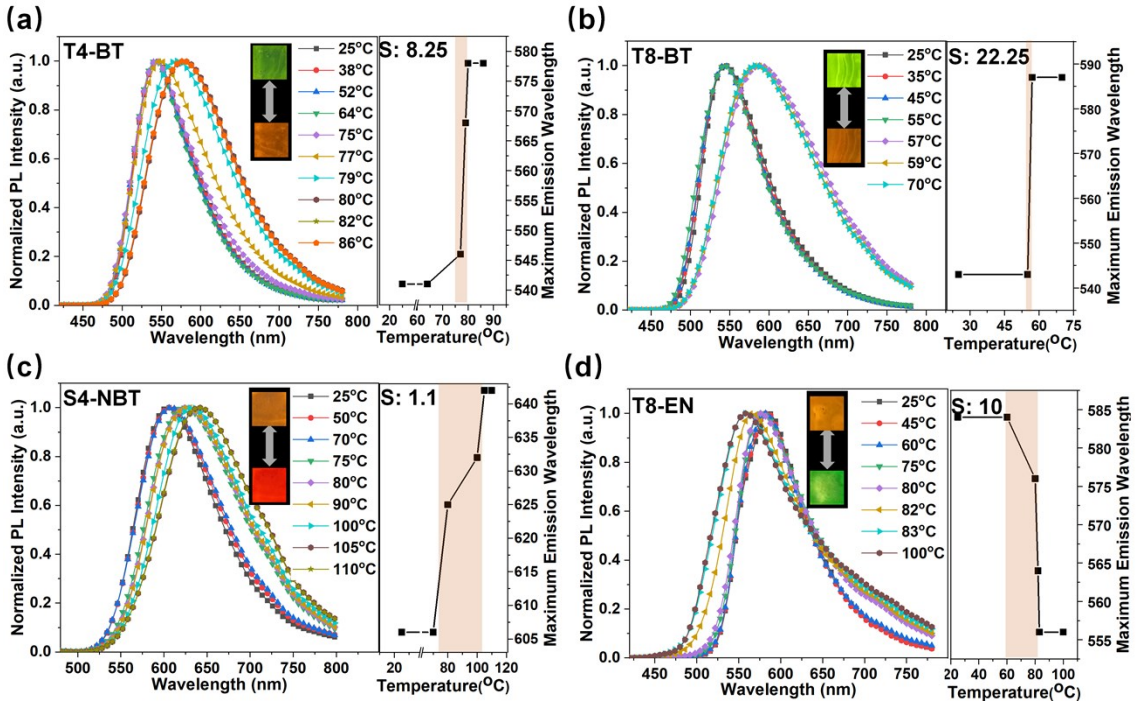

Supplementary Figure 18. The temperature-dependent normalized photoluminescence spectrum and plots of the maximum emission wavelength with temperature of the films of **T4-BT (a)**, **T8-BT (b)**, **S4-NBT (c)** and **T8-EN (d)** upon heating. Insets: photographs of fluorescence changes of compounds in films before (upside) and after (bottom) heating (quartz sheet size: 1 cm * 1 cm). S: sensitivity (nm/ °C).

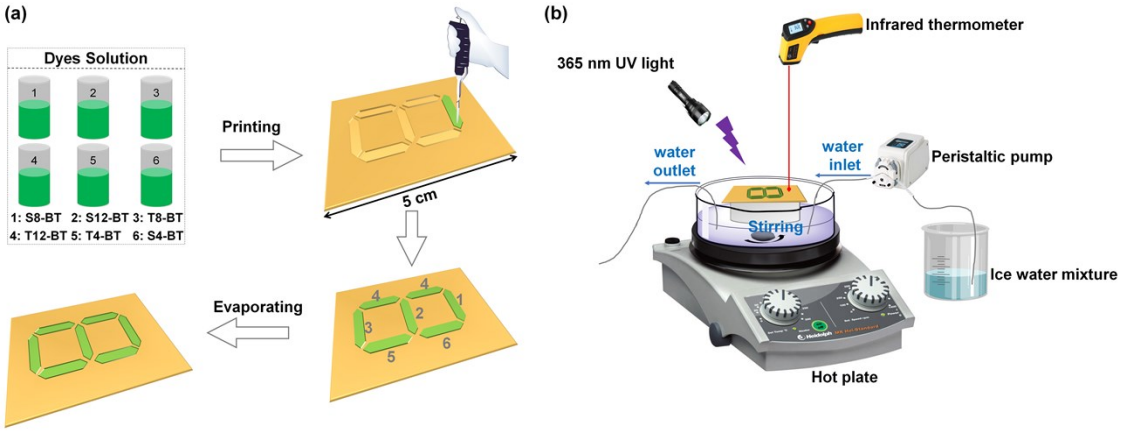

Supplementary Figure 19. Schematic representation of the pattern preparation process **(a)** and the test equipment **(b)** for realizing twelfth-level data encryption application.

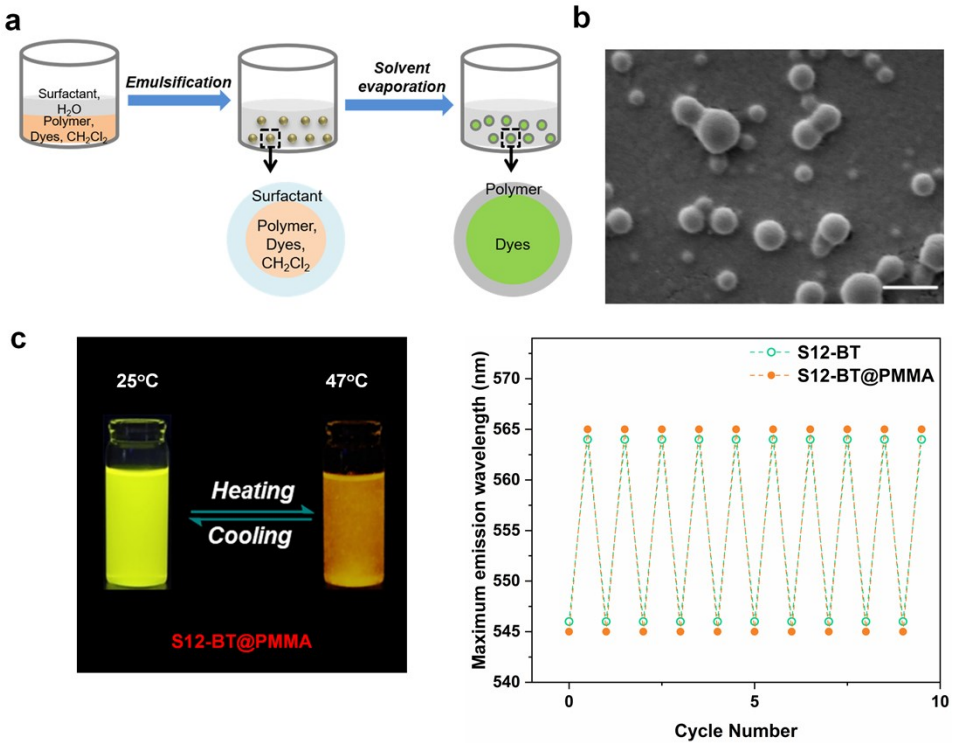

Supplementary Figure 20. (a) Schematic representation of the emulsion-solvent evaporation method. **(b)** SEM image **S12-BT@PMMA** inks (scal bar: 100 nm). **(c)** Digital fluorescence photographs of **S12-BT@PMMA** inks and its thermochromic luminescence reproducibility. All pictures were taken under 365 nm UV light.

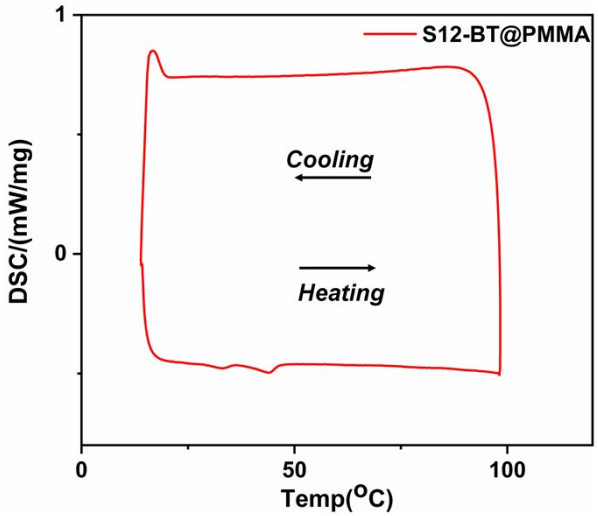

Supplementary Figure 21. DSC curves of **S12-BT@PMMA**.

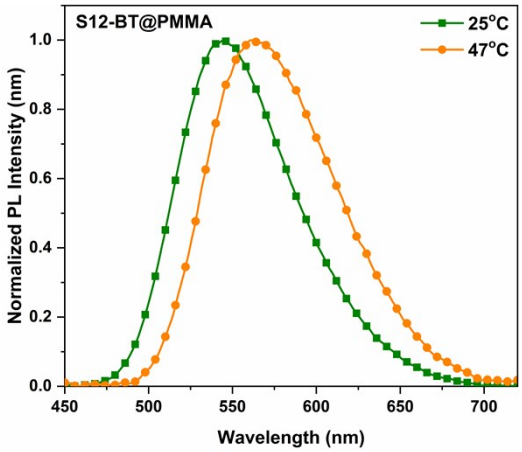

Supplementary Figure 22. Normalized PL spectra of **S12-BT@PMMA** before (green line) and after (yellow line) heating.

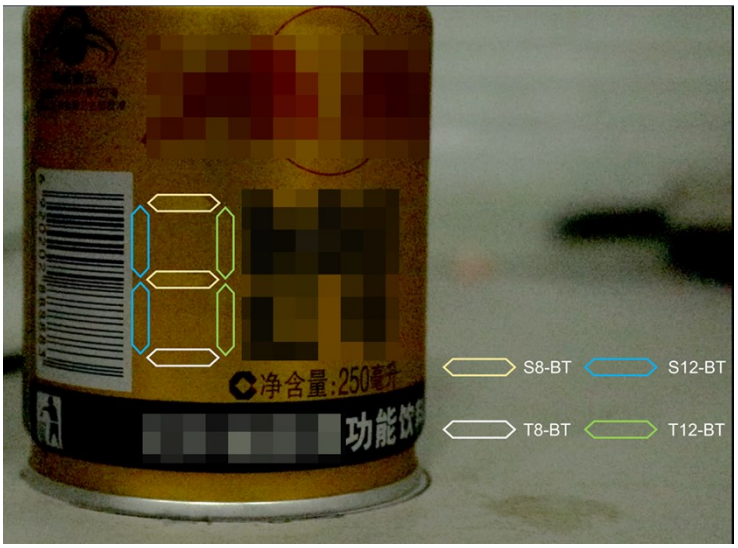

Supplementary Figure 23. Schematic representation for the manipulation of advanced anticounterfeiting applications on zip-pop can using dyes **S8-BT**, **S12-BT**, **T8-BT** and **T12-BT**.

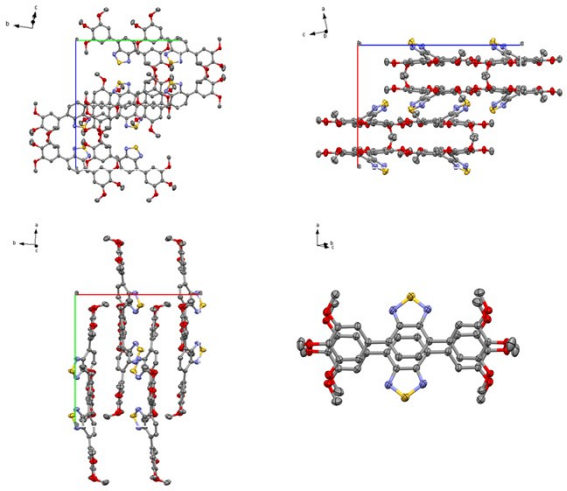

Supplementary Figure 24. Molecular arrangement of the **S1-BT** single crystal. Hydrogen is hidden. (CCDC: 1971259)

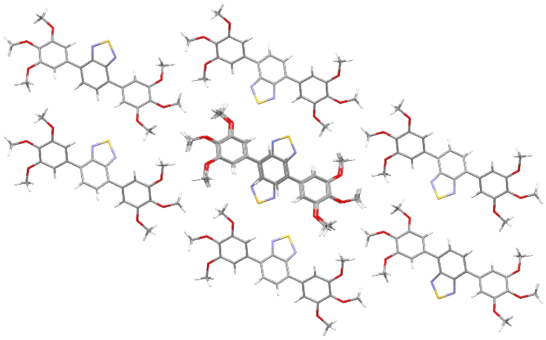

Supplementary Figure 25. Molecular arrangement of the **S1-BT** predicted crystal. Long alkyl chains were replaced by methoxy for efficiency calculation.

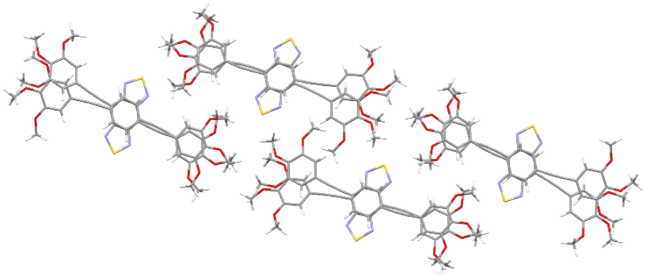

Supplementary Figure 26. Molecular arrangement of the **T12-BT** predicted crystal. Long alkyl chains were replaced by methoxy for efficiency calculation.

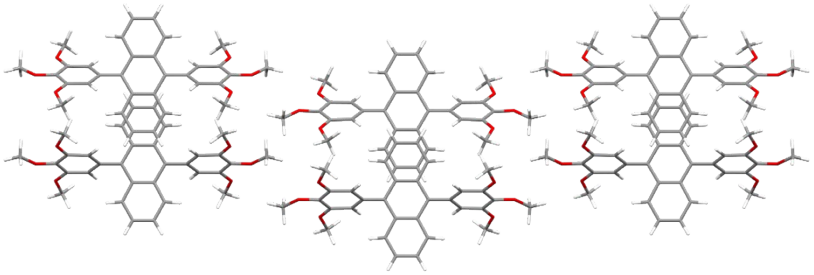

Supplementary Figure 27. Molecular arrangement of the **S12-EN** predicted crystal. Long alkyl chains were replaced by methoxy for efficiency calculation.

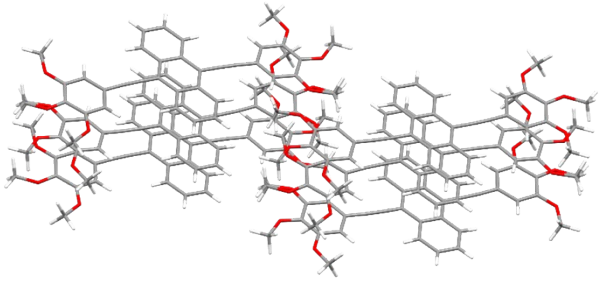

Supplementary Figure 28. Molecular arrangement of the **T12-EN** predicted crystal. Long alkyl chains were replaced by methoxy for efficiency calculation.

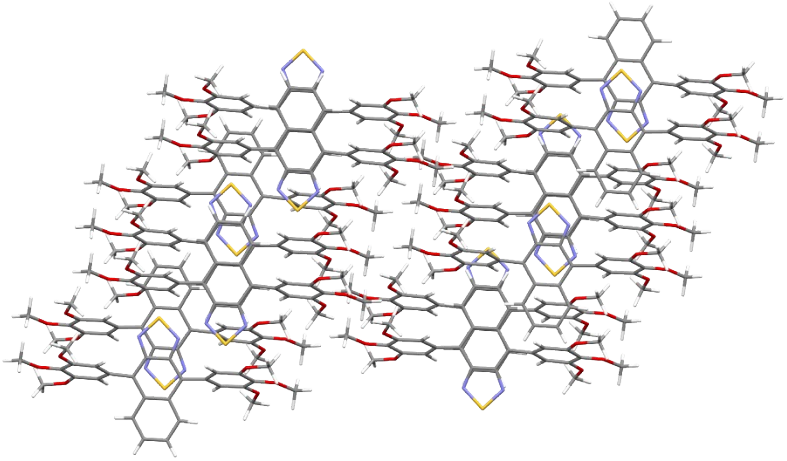

Supplementary Figure 29. Molecular arrangement of the **S12-NBT** predicted crystal. Long alkyl chains were replaced by methoxy for efficiency calculation.

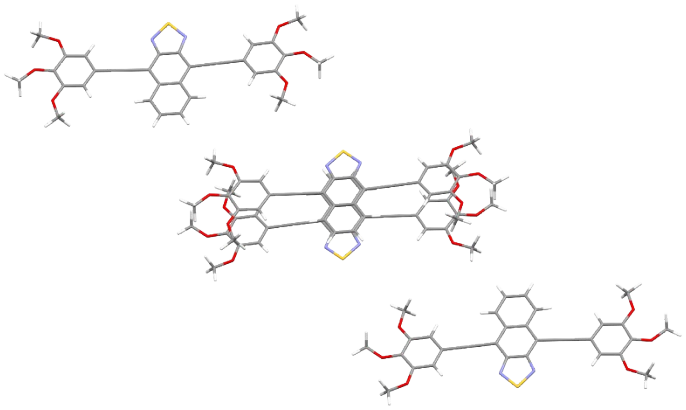

Supplementary Figure 30. Molecular arrangement of the **T12-NBT** predicted crystal. Long alkyl chains were replaced by methoxy for efficiency calculation.

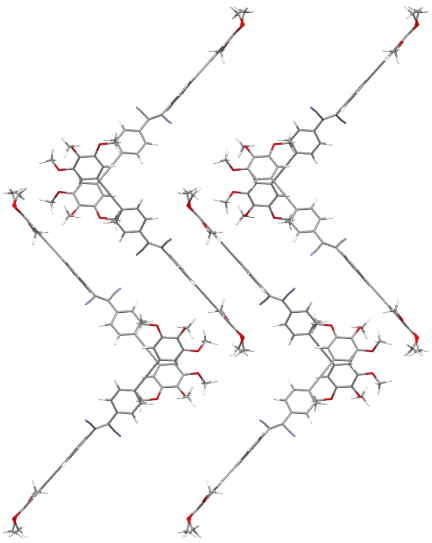

Supplementary Figure 31. Molecular arrangement of the **T12-CN** predicted crystal. Long alkyl chains were replaced by methoxy for efficiency calculation.

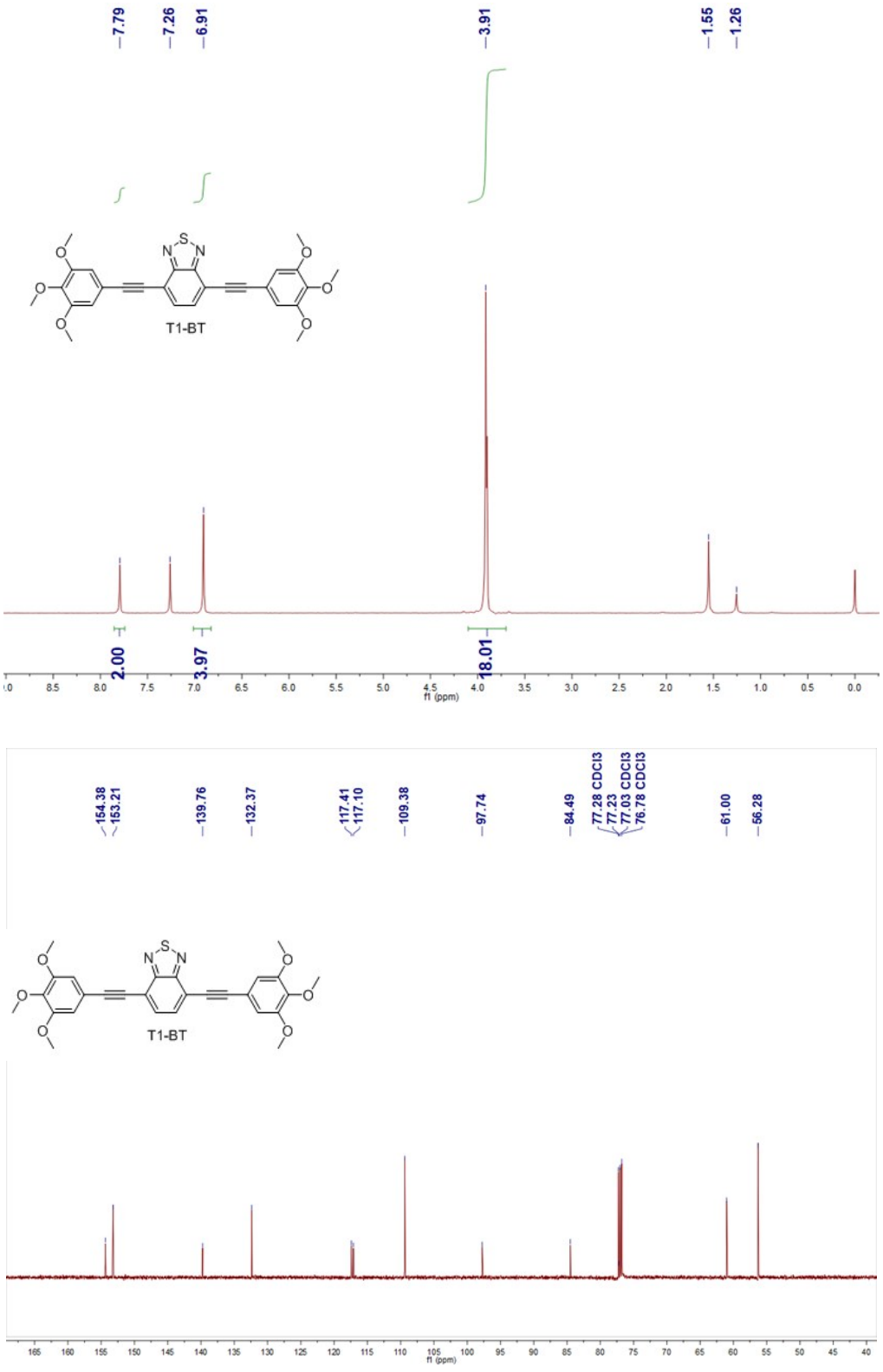

Supplementary Figure 32. ^{1}H NMR (up) and ^{13}C NMR (bottom) spectrum of **T1-BT** in $CDCl_3$.

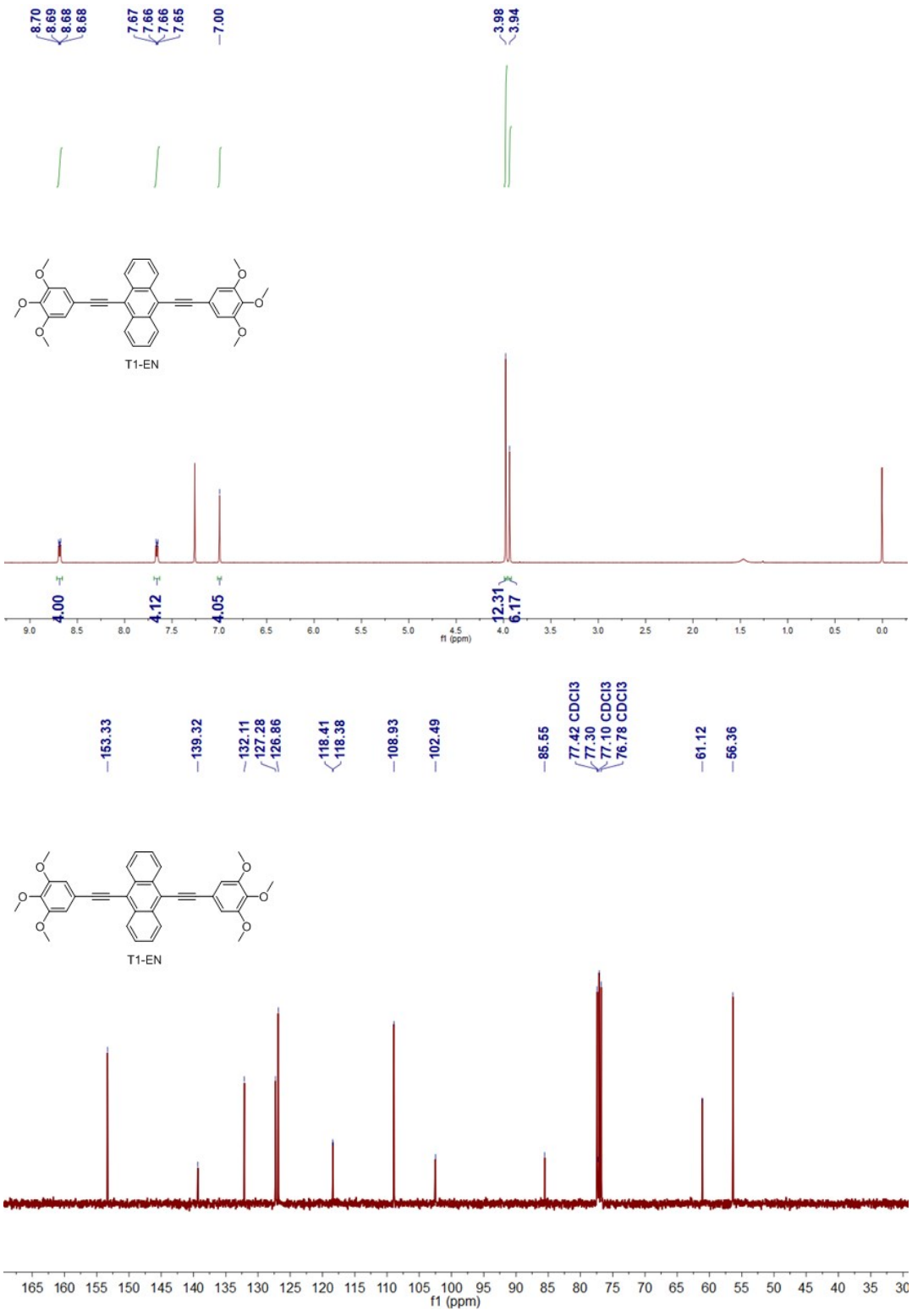

Supplementary Figure 33. ^{1}H NMR (up) and ^{13}C NMR (bottom) spectrum of **T1-EN** in $CDCl_3$.

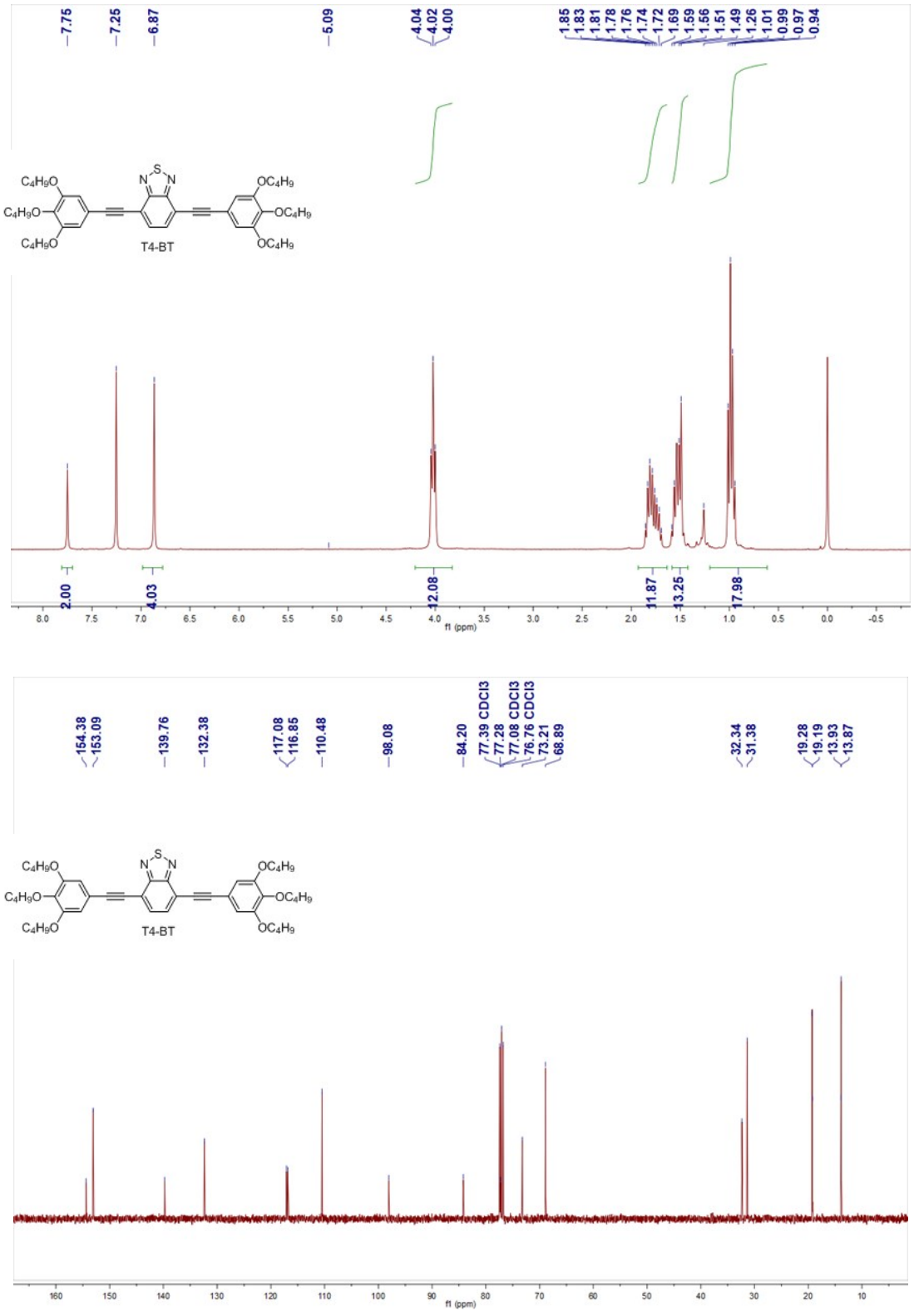

Supplementary Figure 34. ^{1}H NMR (up) and ^{13}C NMR (bottom) spectrum of **T4-BT** in $CDCl_3$.

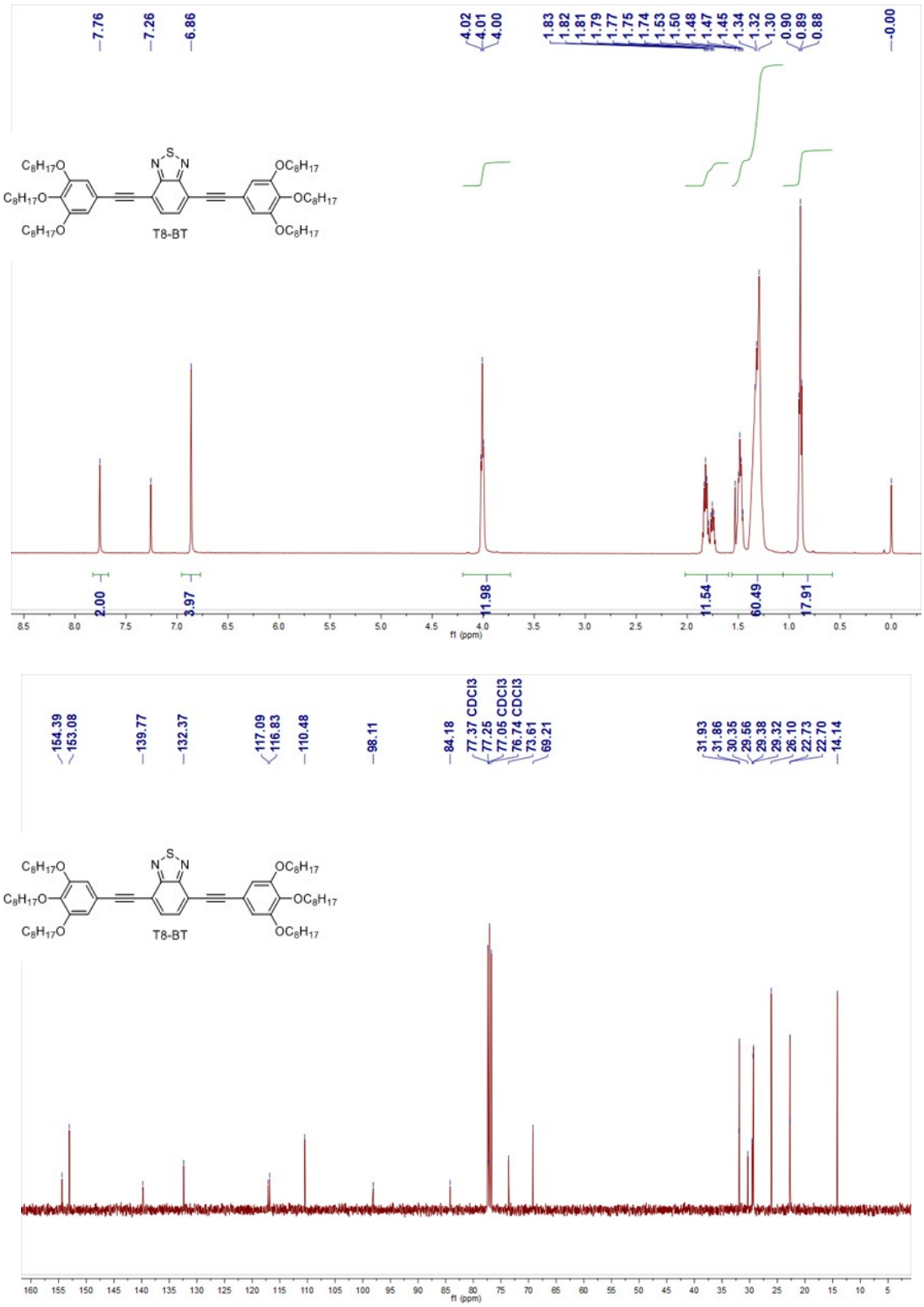

Supplementary Figure 35. ^{1}H NMR (up) and ^{13}C NMR (bottom) spectrum of **T8-BT** in $CDCl_3$.

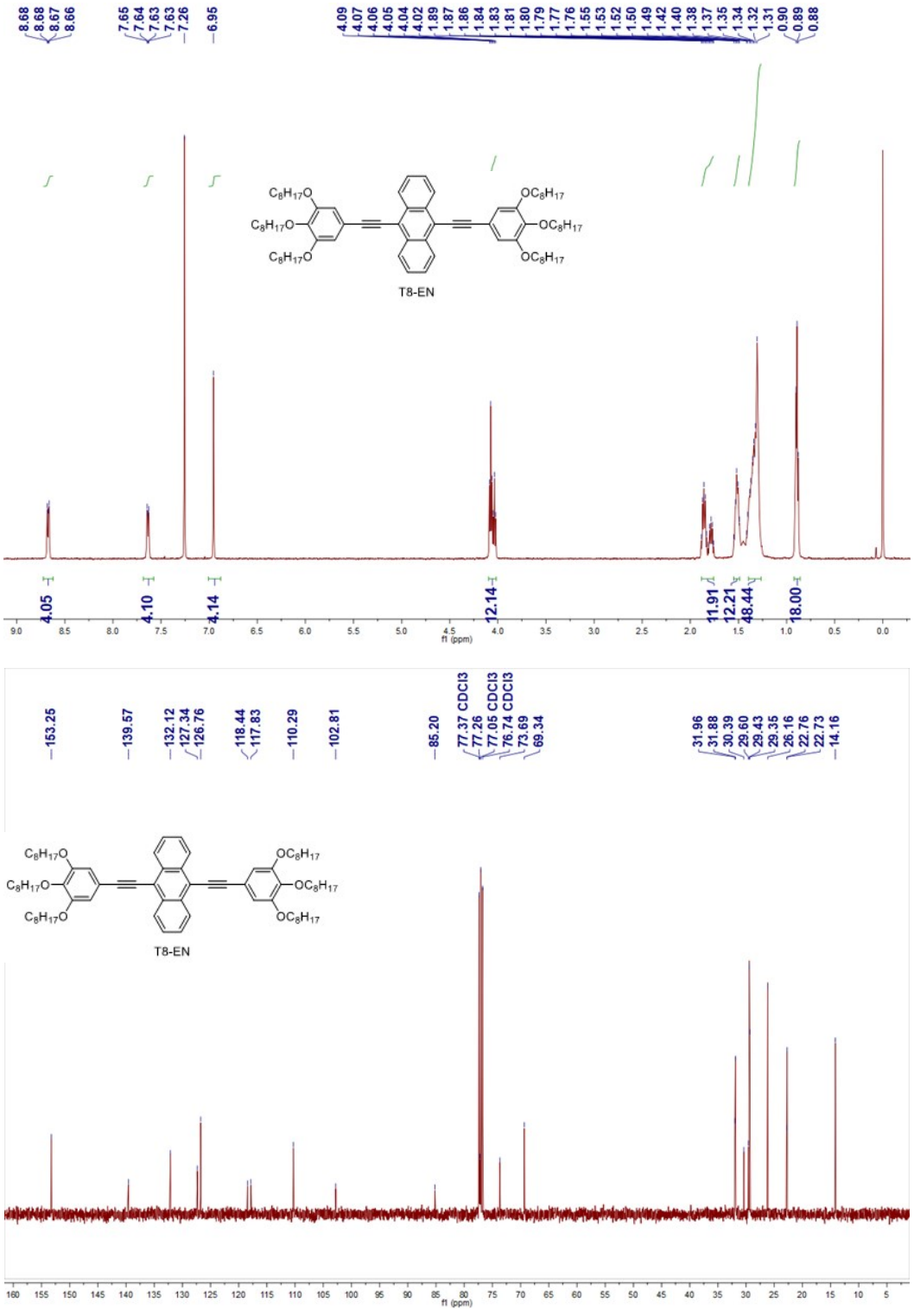

Supplementary Figure 36. ^{1}H NMR (up) and ^{13}C NMR (bottom) spectrum of **T8-EN** in $CDCl_3$.

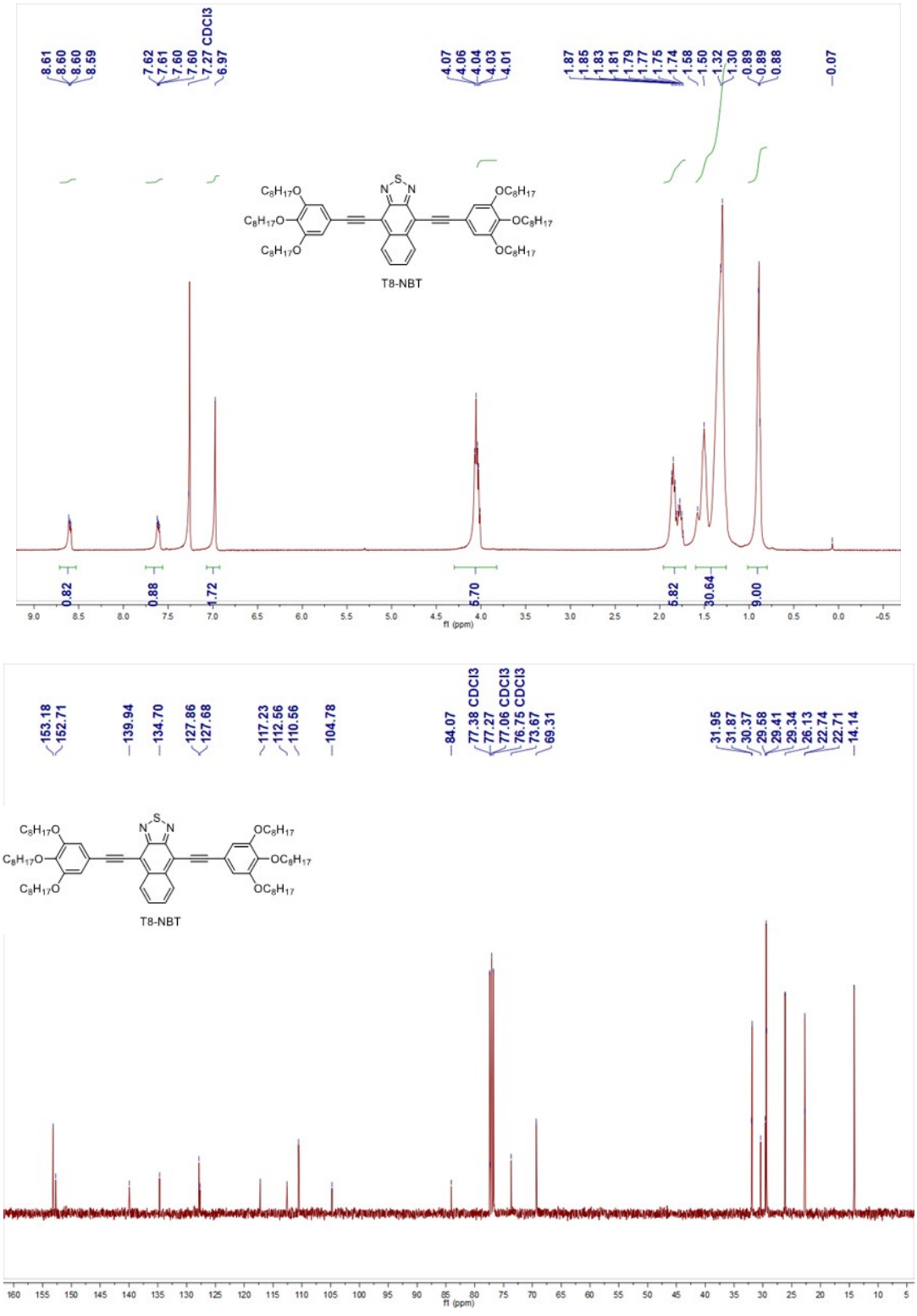

Supplementary Figure 37. ^{1}H NMR (up) and ^{13}C NMR (bottom) spectrum of **T8-NBT** in $CDCl_3$.

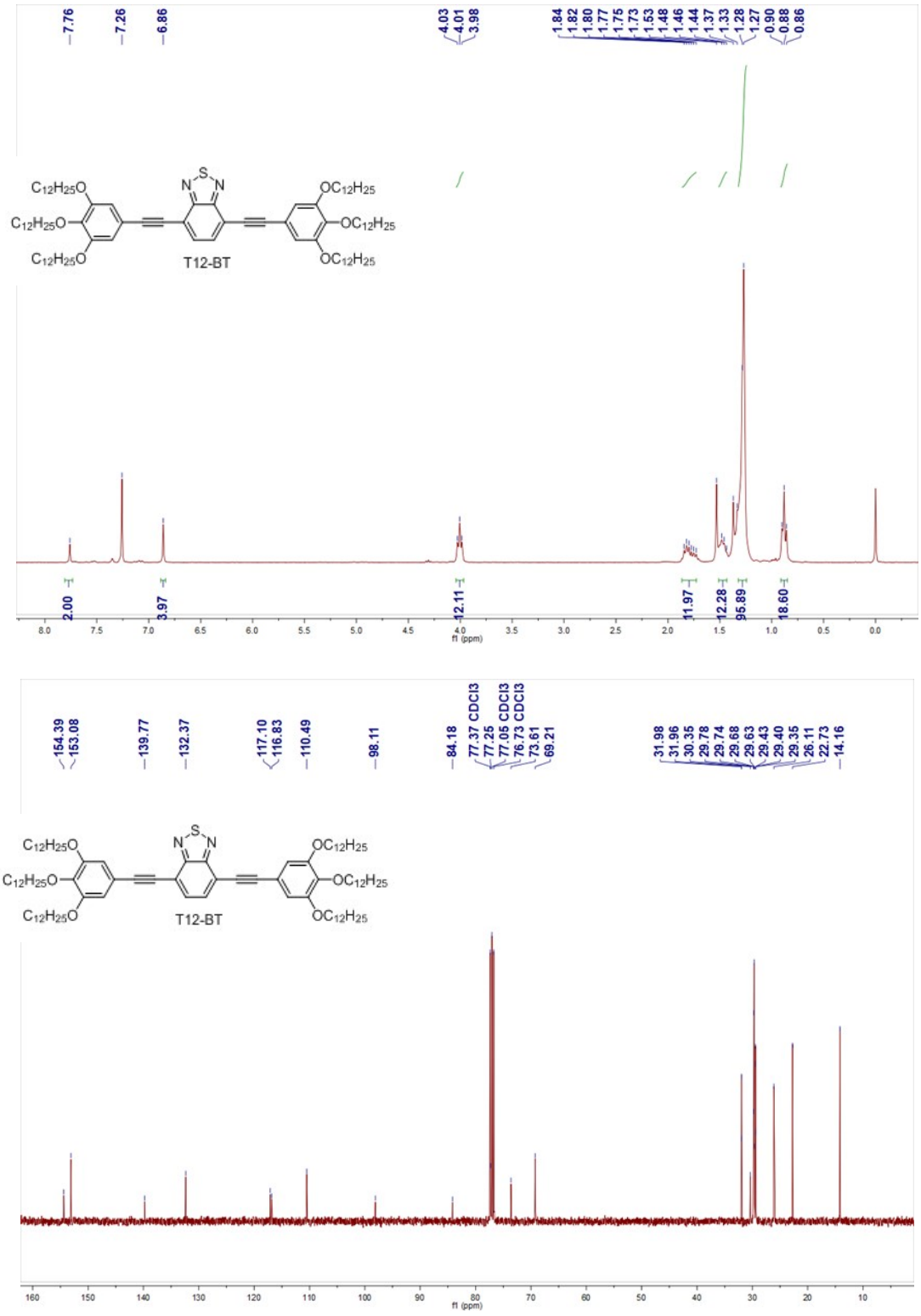

Supplementary Figure 38. ^{1}H NMR (up) and ^{13}C NMR (bottom) spectrum of **T12-BT** in $CDCl_3$.

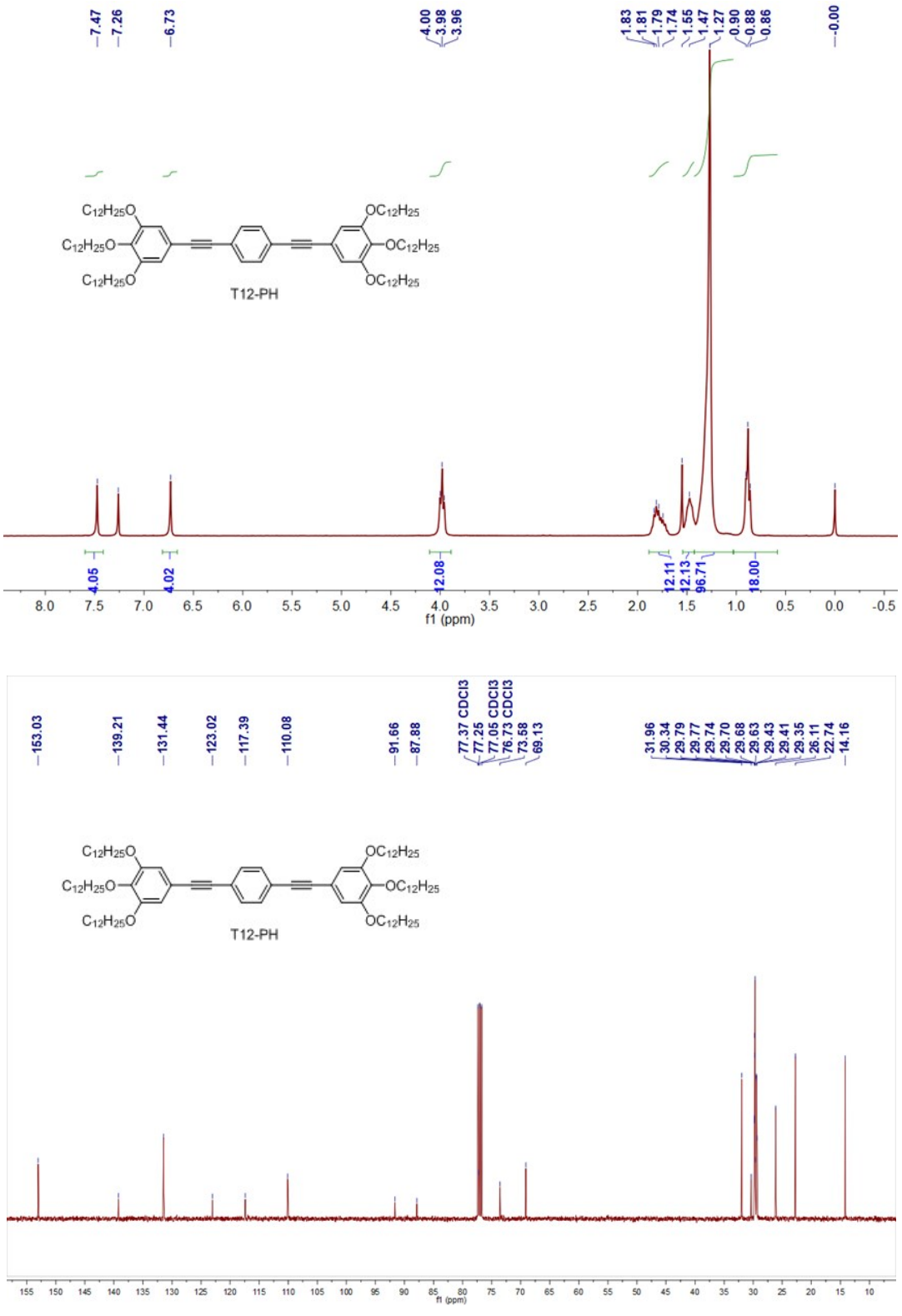

Supplementary Figure 39. ^{1}H NMR (up) and ^{13}C NMR (bottom) spectrum of **T12-PH** in $CDCl_3$.

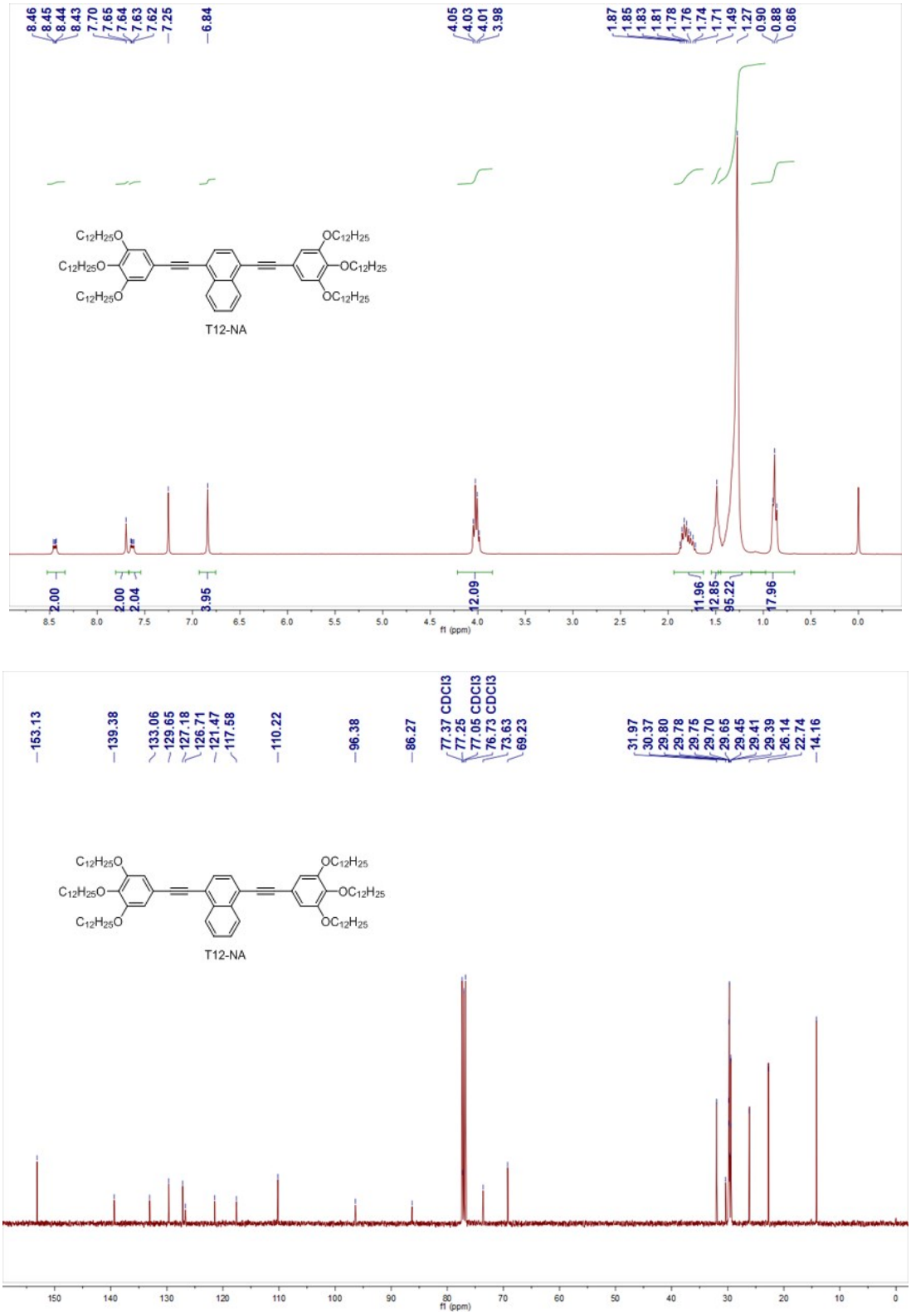

Supplementary Figure 40. ^{1}H NMR (up) and ^{13}C NMR (bottom) spectrum of **T12-NA** in $CDCl_3$.

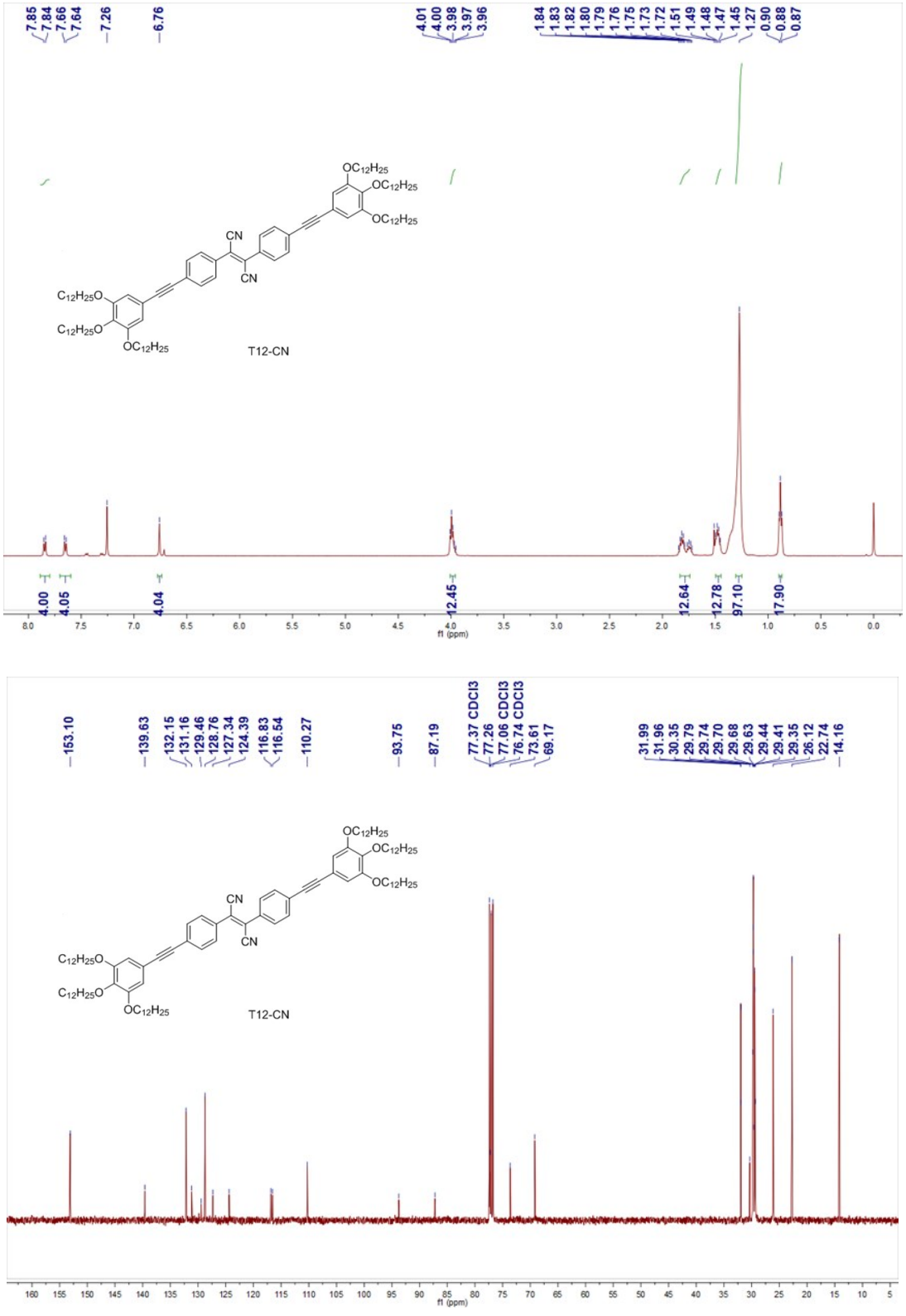

Supplementary Figure 41. ^{1}H NMR (up) and ^{13}C NMR (bottom) spectrum of **T12-CN** in $CDCl_3$.

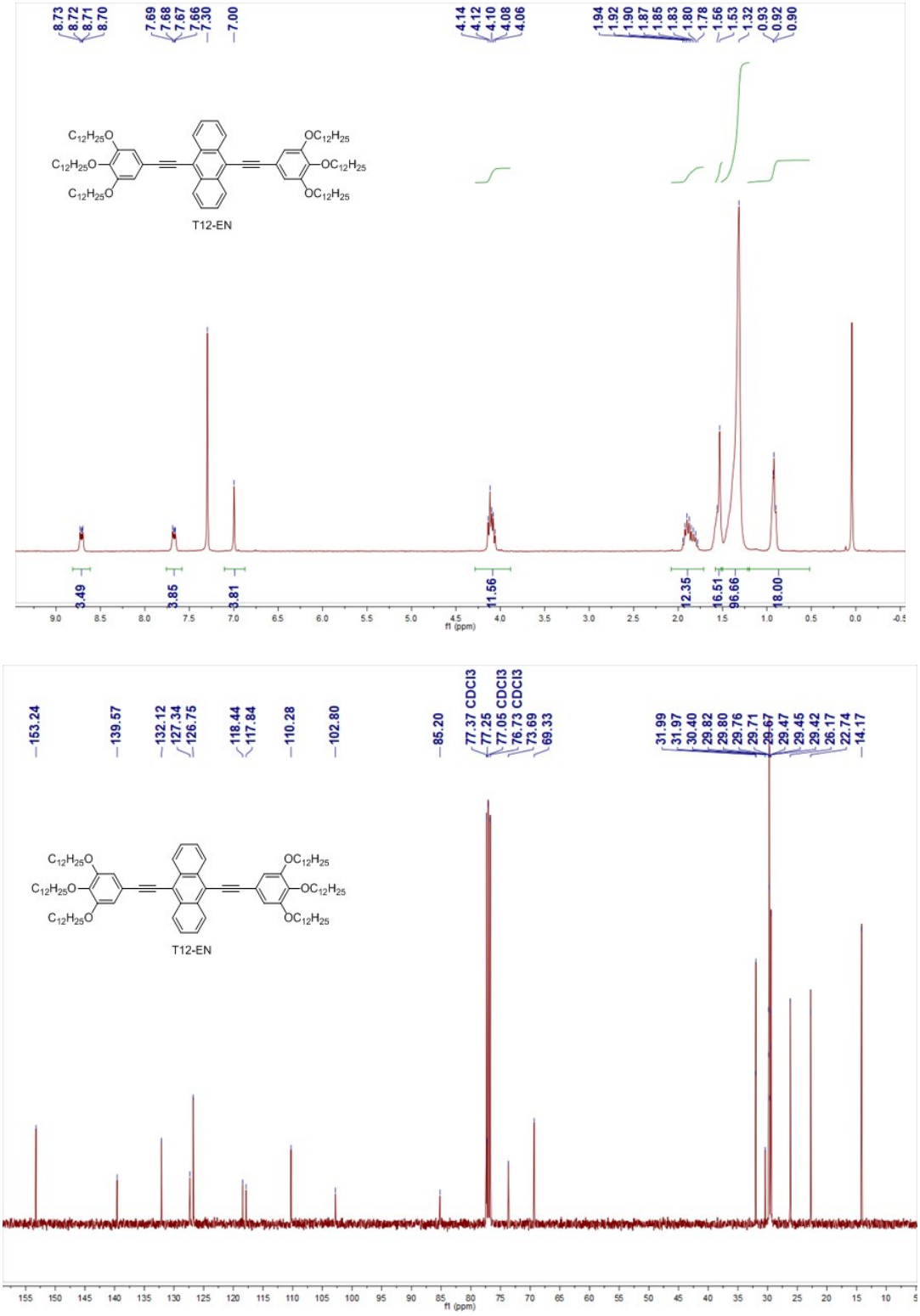

Supplementary Figure 42. ^{1}H NMR (up) and ^{13}C NMR (bottom) spectrum of **T12-EN** in $CDCl_3$.

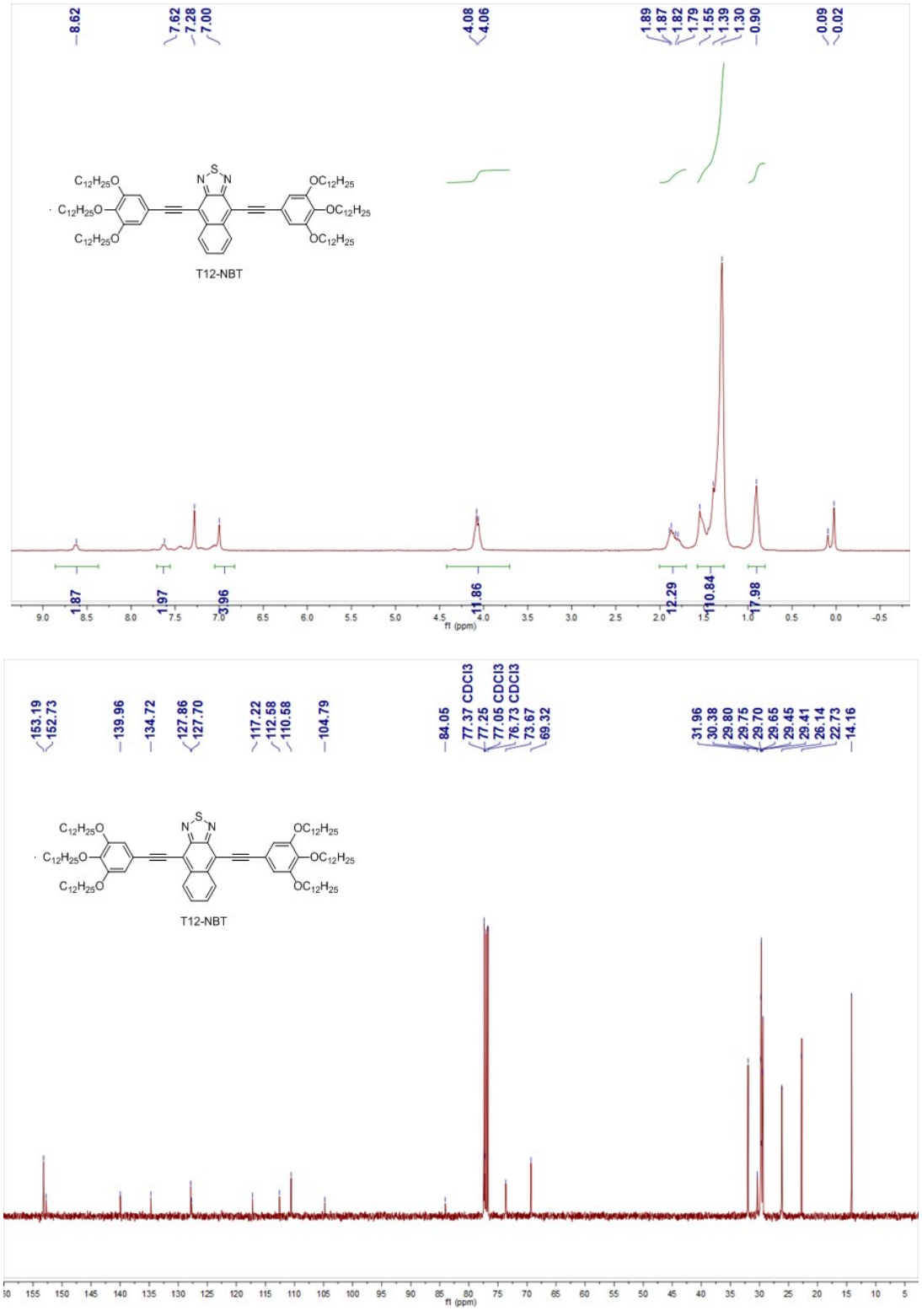

Supplementary Figure 43. ^{1}H NMR (up) and ^{13}C NMR (bottom) spectrum of **T12-NBT** in $CDCl_3$.

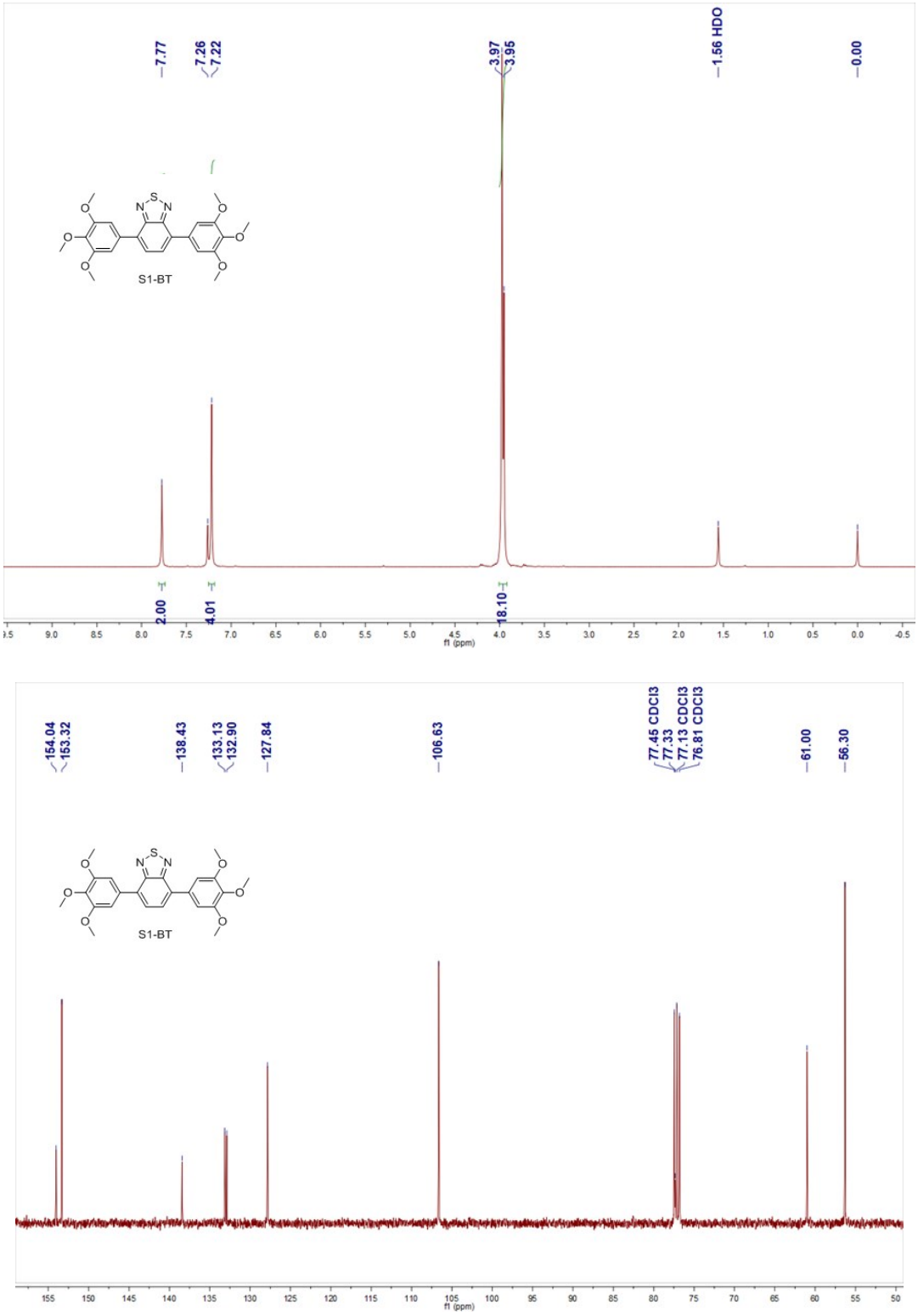

Supplementary Figure 44. ^{1}H NMR (up) and ^{13}C NMR (bottom) spectrum of **S1-BT** in $CDCl_3$.

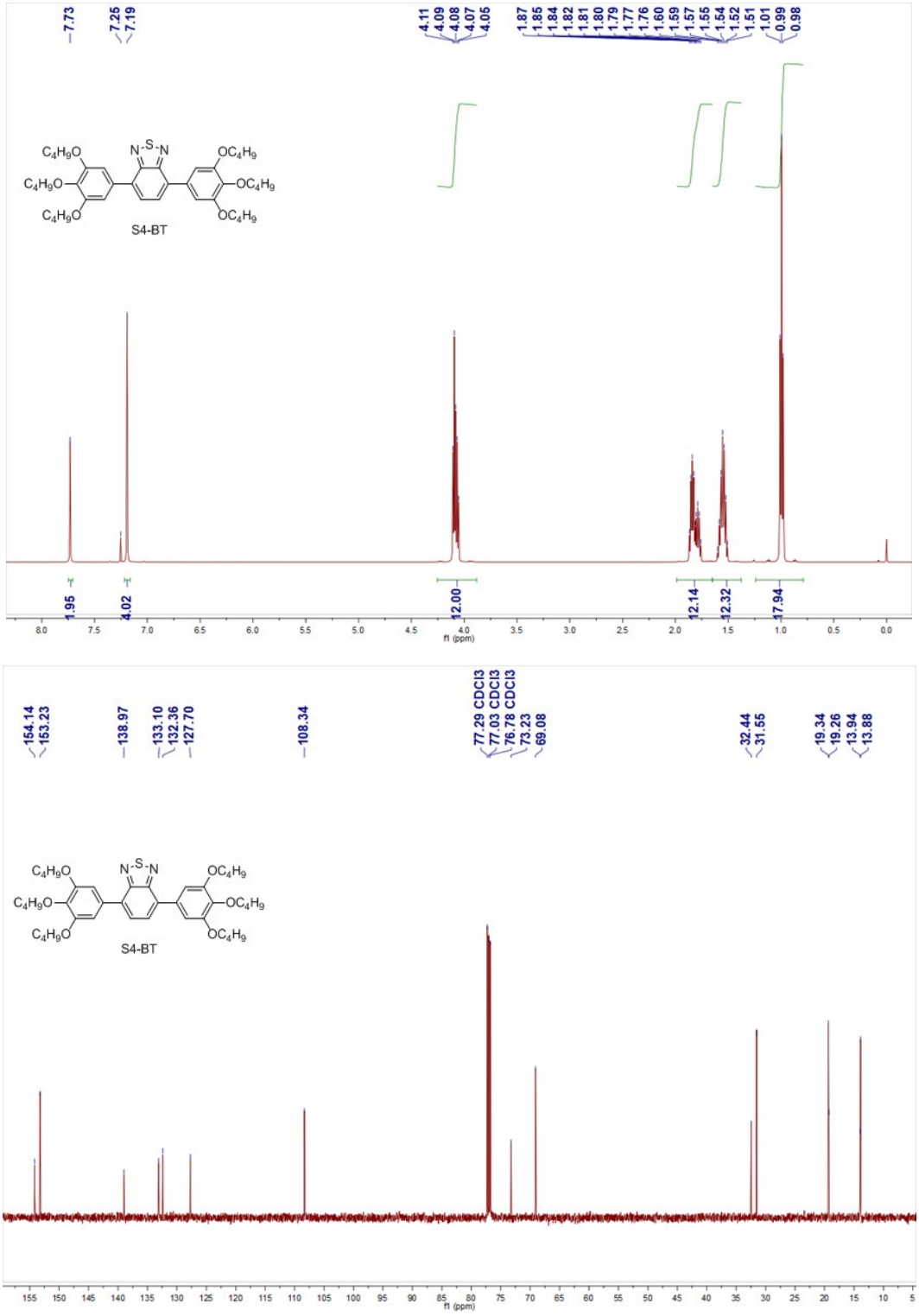

Supplementary Figure 45. ^{1}H NMR (up) and ^{13}C NMR (bottom) spectrum of **S4-BT** in $CDCl_3$.

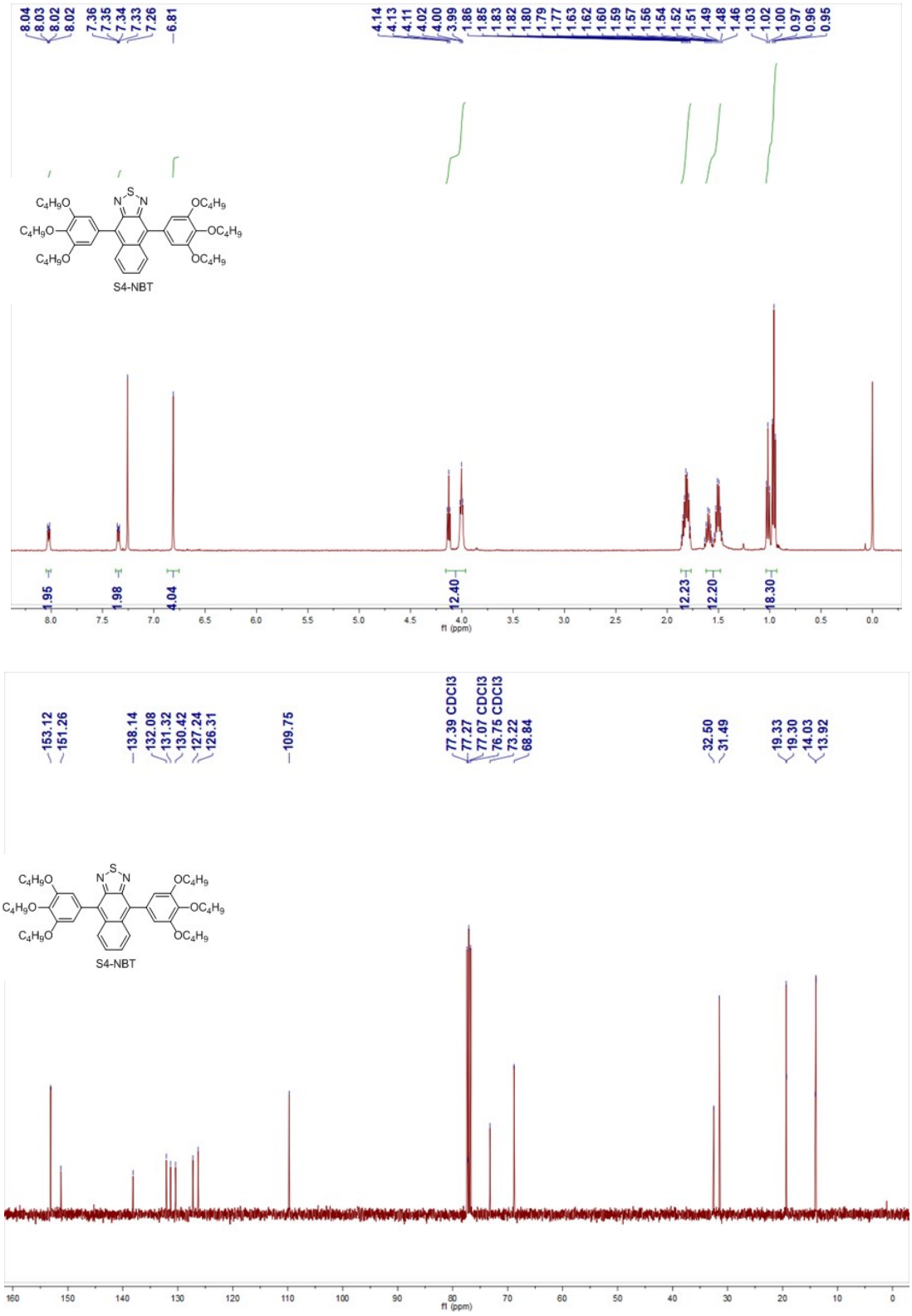

Supplementary Figure 46. ^{1}H NMR (up) and ^{13}C NMR (bottom) spectrum of **S4-NBT** in $CDCl_3$.

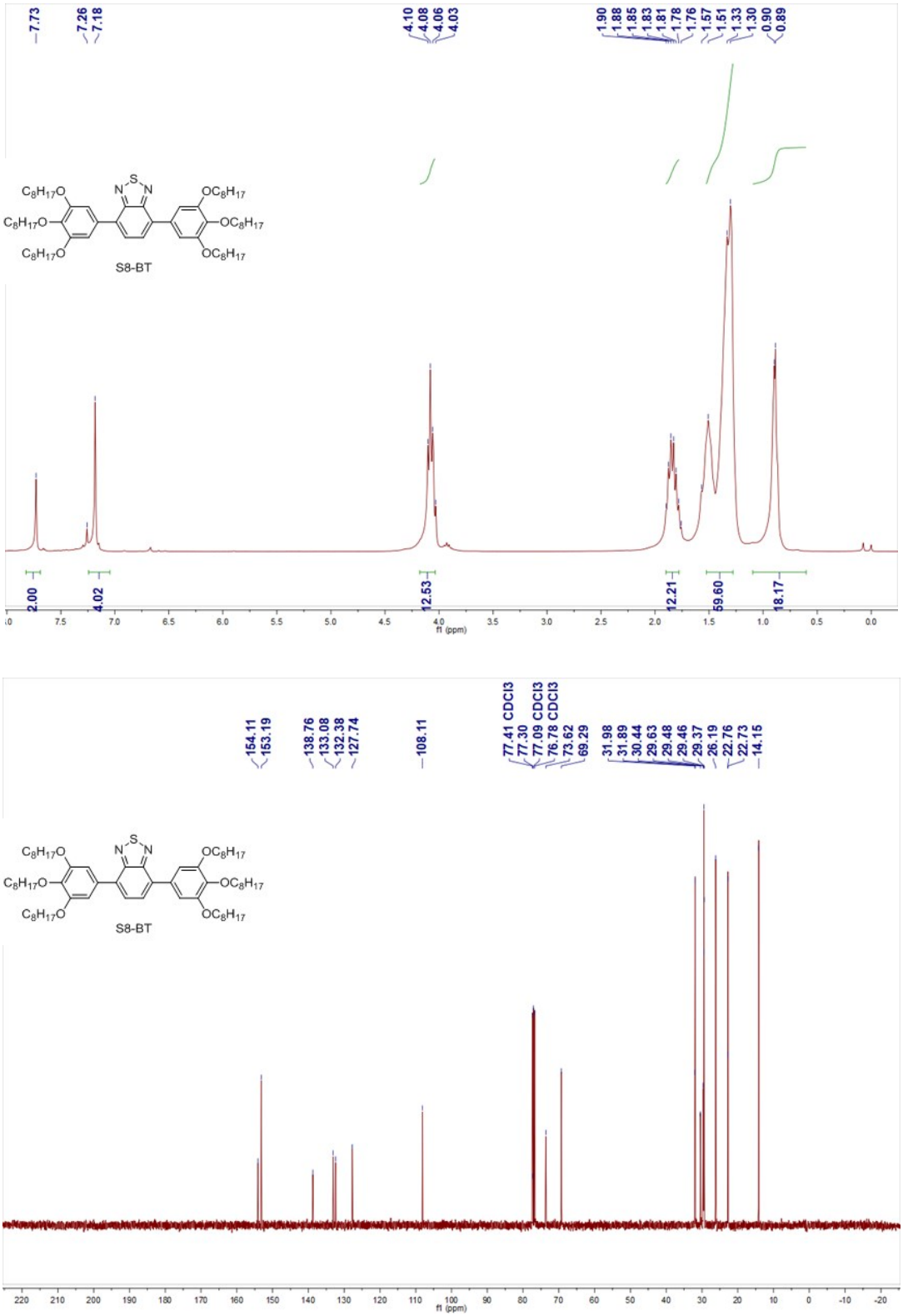

Supplementary Figure 47. ^{1}H NMR (up) and ^{13}C NMR (bottom) spectrum of **S8-BT** in $CDCl_3$.

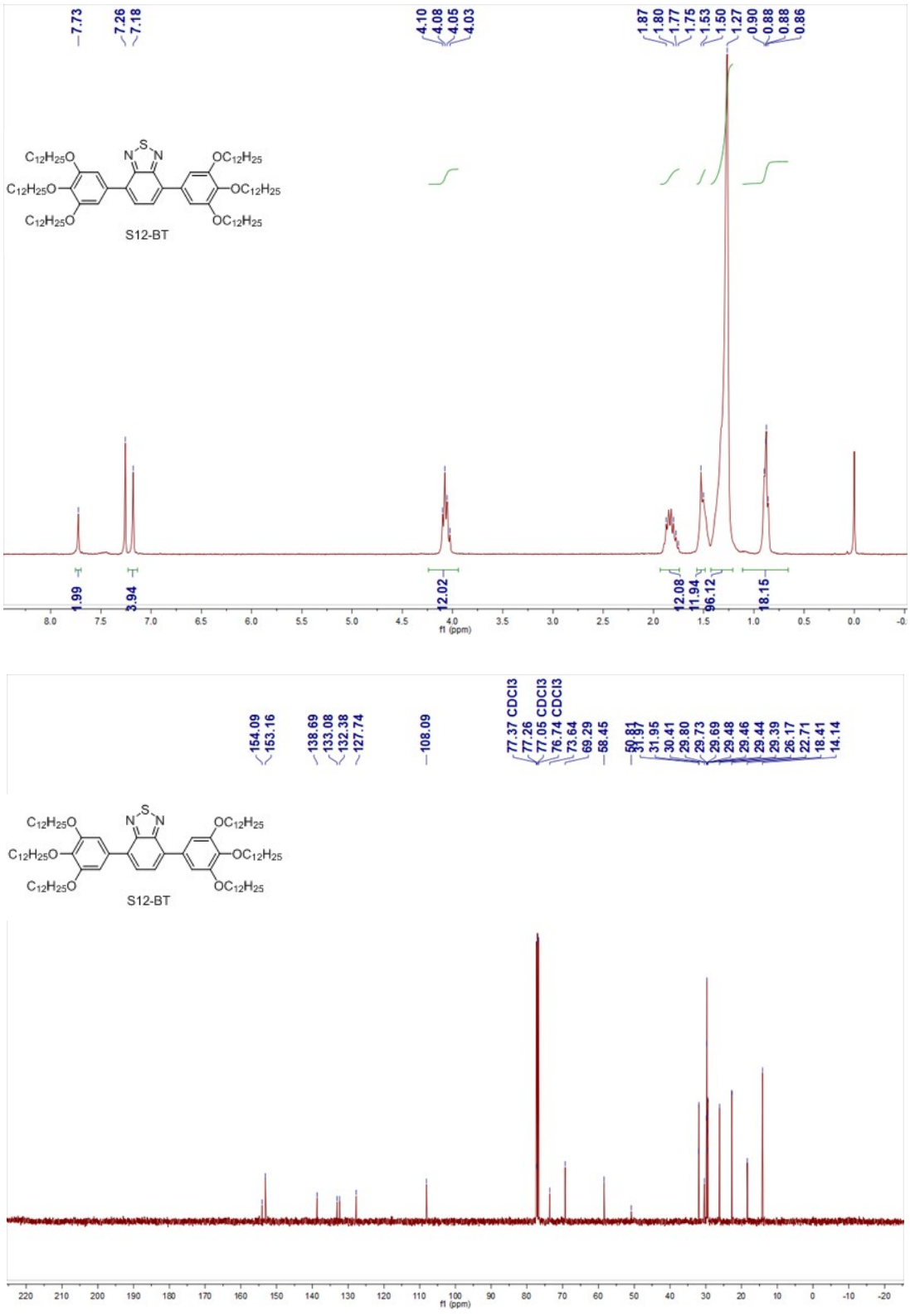

Supplementary Figure 48. ^{1}H NMR (up) and ^{13}C NMR (bottom) spectrum of **S12-BT** in $CDCl_3$.

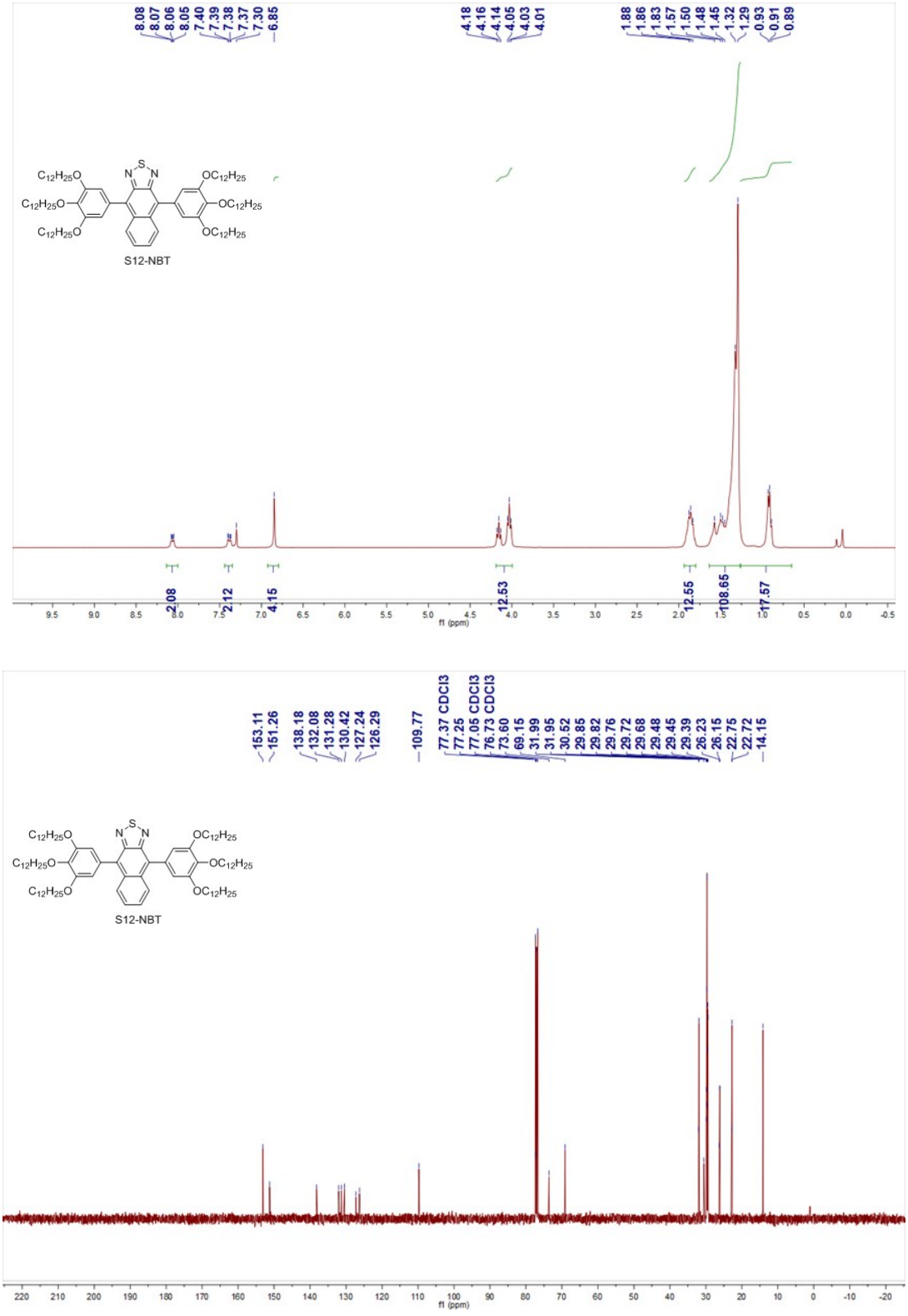

Supplementary Figure 49. ^{1}H NMR (up) and ^{13}C NMR (bottom) spectrum of **S12-NBT** in $CDCl_3$.

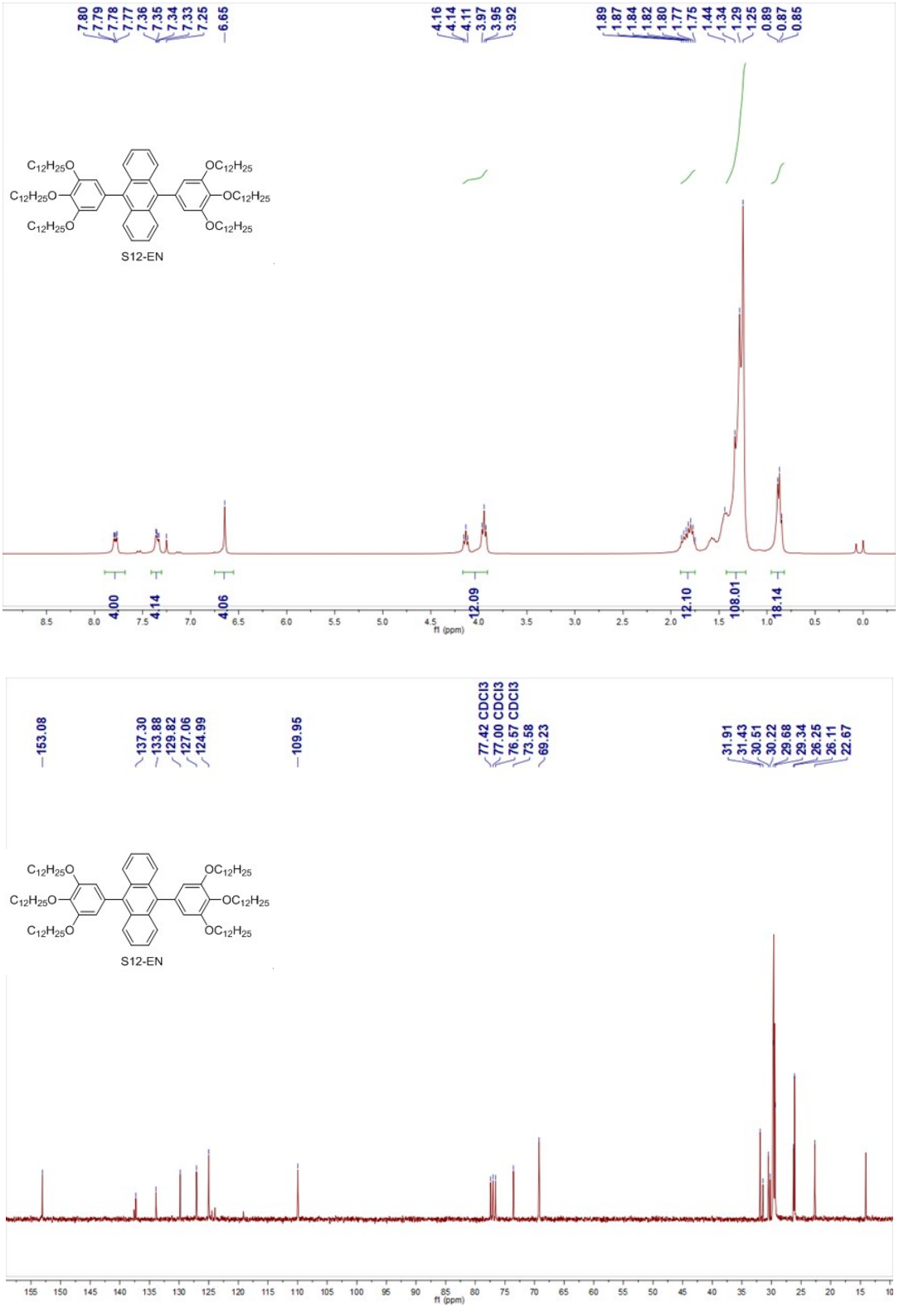

Supplementary Figure 50. ^{1}H NMR (up) and ^{13}C NMR (bottom) spectrum of **S12-EN** in $CDCl_3$.

Table S1. Photophysical properties of thermochromic luminophores

	λ_{abs} (nm)	Solution		Solid		T_m (°C)
		Hexane	DCM	λ_{rt} (nm)	λ_m (nm)	
S1-BT	283, 405	536	570	545	576	190
S4-BT	285, 408	538	576	546	595	85
S8-BT	283, 406	537	575	546	603	35
S12-BT	284, 411	539	579	559	577	47
T4-BT	310, 437	518	584	553	570	80
T8-BT	312, 438	519	582	542	570	56
T12-BT	310, 437	510	584	532	569	60
S4-NBT	352, 495	595	610	622	642	85
S12-NBT	350, 492	593	612	629	653	54
T12-NBT	271, 346, 554	616	658	666	704	68
T12-PH	337	-	413	435, 536	416, 525	58
T12-NA	373	410	445	458	458	45
S12-EN	357, 375, 395	421	434	459	439	53
T8-EN	316, 451, 475	493	505	599	558	80
T12-EN	319, 453, 472	490	503	522	571	72
T12-CN	293, 410	-	-	581	585	68

Table S2. Crystallographic data

	S1-BT
Formula	$C_{24}H_{24}N_2O_6S$
Molecular weight	468.51
Temperature (K)	298
Space group	*P b c a*
Hall group	-P 2ac 2ab
a (Å)	14.6959(11)
b (Å)	15.6387(11)
c (Å)	19.4963(14)
α (º)	90.0000
β (º)	90.0000
γ (º)	90.0000
Volume (Å^3)	4480.7(6)
Z	8
ρ_{calcd} (g cm^{-3})	1.395
Mu (mm-1)	0.189
F000	1968.0
F000'	1969.96
h, k, lmax	22, 23, 29
Nref	7851
CCDC	1971259

Supplementary References

1. R. Martin, P. Prieto, J. R. Carrillo, A. M. Rodriguez, A. Cozar, P. G. Boj, M. A. Garcia, M. G. Ramirez, *J. Mater. Chem. C,* 2019, **7**, 9996-10007.

2. R. Greiner, T. Schluecker, D. Zgela, H. Langhals, *J. Mater. Chem. C,* 2016, **4**, 11244-11252.

3. H. Taing, A. M. Cassar, M. U. Ocheje, S. Rondeau-Gagne, T. H. El-Assaad, C. A. Sharabati, B. R. Kaafarani, S. H. Eichhorn, *Chempluschem,* 2019, **84**, 103-106.

4. M. Jasinski, K. Szymanska, A. Gardias, D. Pociecha, H. Monobe, J. Szczytko, P. Kaszynski, *Chemphyschem,* 2019, **20**, 636-644.

5. H. Wu, Z. Chen, W. Chi, A. K. Bindra, L. Gu, C. Qian, B. Wu, B. Yue, G. Liu, G. Yang, L. Zhu, Y. Zhao, *Angew. Chem. Int. Ed.,* 2019, **58**, 11419-11423.